이학박사 학위 논문

CRISPR-매개 염기 편집 개선을 위한 소분자 약물 스크리닝

Small molecule drug screening to improve CRISPR-mediated base editing

울 산 대 학 교 대 학 원

의 과 학 과

신 하 림

Small molecule drug screening to improve CRISPR-mediated base editing

지 도 교 수 김 용 섭

이 논문을 이학박사학위 논문으로 제출함

2023 년 8 월

울 산 대 학 교 대 학 원

의 과 학 과

신 하 림

신하림의 이학박사학위 논문을 인준함

심사위원 신 동 명(인)

심사위원 성 영 훈(인)

심사위원 최 경 철(인)

심사위원 김 용 섭(인)

심사위원 김 헌 석(인)

울 산 대 학 교 대 학 원

2023 년 8 월

ABSTRACT

The clustered regularly interspaced short palindromic repeats (CRISPR)-*CRISPR*-associated protein 9 (Cas9) system, which was originally designed as an adaptive immune system to defend against viral genomes, is now more commonly known as a genome editing tool termed RNA-guide engineered nucleases (RGENs). The mechanism of the CRISPR-Cas9 system is that Cas9 protein and gRNA form a complex, recognize a target DNA sequence, and induce a DNA double-strand break (DSBs). Cleaved DNA is repaired through an intracellular DNA repair pathway, non-homologous end joining (NHEJ), or homology-directed repair (HDR). NHEJ induces gene disruption through small insertions and deletions, whereas HDR induces homologous recombination in the presence of a donor template, thus assisting with gene correction and insertion. Recently, CRISPR-based genome editing has applications in a variety of fields, including agriculture, drug discovery, medicine, and biotechnology. Especially it is attracting attention as a promising tool to treat disease, and clinical trial development is currently accelerating. However, despite having enormous potential for treating disease, there are several problems. Recently, p53-mediated toxicity, large chromosomal deletions and rearrangements, and the occurrence of unwanted byproducts and indels caused by DSBs caused by Cas9-based genome editing have been continuously reported. In addition, since many pathogenic genetic diseases are caused by point mutations, Cas9 nuclease-based disease-related mutation

correction is inefficient and has safety issues. In this manner, an approach to precisely correct the target base was required, prompting the development of a base editor capable of correcting the base without DSBs. Base editors currently have two major types, cytosine base editor (CBE) and adenine base editor (ABE). CBE fused with cytidine deaminase to nCas9 (nickase Cas9, catalytically inactive D10A mutation) induces C:G to T:A conversion and ABE fused with adenine deaminase to nCas9 induces A:T to G:C conversion. The present generation of base editors has evolved and refined to optimize efficiency; however, their activity is highly variable depending on cell type and target sequences. Previous studies have demonstrated an attempt to improve the efficiency of the base editor. Notably, the efficiency of CBE was improved by fusing uracil glycosylase inhibitor (UGI) which inhibits the activity of uracil N-glycosylase (UNG). Therefore, this study aimed to investigate the effect of inhibition of certain endogenous protein functions of base editors. To inhibit certain protein functions, small molecule drugs have been adopted, and these strategies have been used to improve the efficiency of Cas9-based genome editing but have not been investigated in base editors. In this study, a fluorescence-based reporter system was developed to identify novel small molecules. 414 small molecule drug libraries were screened in the HAP1 cell line, which was integrated with a reporter system, and histone deacetylase (HDAC) inhibitors were ranked high. Romidepsin with the highest-ranking increased adenine base editing efficiency up to 3.8-fold at the endogenous target sites. These effects verified that romidepsin enhances the expression levels of ABE7.10 protein and gRNA. Additionally, HDAC inhibitors can convert euchromatin through histone

hyperacetylation. To evaluate the effect of chromatin status on base editing efficiency, ABE7.10 ribonucleoprotein (RNP), a complex of purified ABE7.10 protein and gRNA that excludes expression-enhancing effect, was electroporated, and romidepsin increased the adenine base editor efficiency up to 4.9-fold. These results suggest that chromatin was converted to an open state throughout the ChIP assay, leading to improved adenine base editing efficiency due to improved RNP accessibility. In conclusion, the HDAC inhibitor can increase the efficiency of CRISPR-mediated base editing based on enhanced expression and improved RNP accessibility. These results may provide insights into further studies to improve the efficiency of CRISPR-mediated genome editing and support strategies to increase the efficiency of in vivo genome editing in therapeutic applications.

Key words: CRISPR, Base editing, Adenine base editor, HDAC inhibitor, romidepsin

CONTENTS

ABSTRACT · · · i

LIST OF FIGURES · · · vii

LIST OF TABLES · · · ix

1. INTRODUCTION · · · 1

2. MATERIALS AND METHODS · · · 7

2.1 Plasmid DNA preparation · · · 7

2.2 Cell culture · · · 8

2.3 HAP1−ABE^{Dox} : EGFP reporter cell line generation · · · 8

2.4 Drug screening · · · 9

2.5 HDAC1 and HDAC2 knockdown cell line generation · · · 10

2.6 Protein purification · · · 11

2.7 Transfection and drug treatment · · · 12

2.8 Targeted deep sequencing and data analysis · · · 13

2.9 Protein expression level measurement · 13

2.10 Quantitative PCR · 14

2.11 Chromatin immunoprecipitation (ChIP) assay · · · · · · · · · · · · · · · · 15

3. RESULTS · 16

3.1 Generation of HAP1−ABE^{Dox} : EGFP cell line · · · · · · · · · · · · · · · · 16

3.2 Small molecule drug screening to improve adenine base editing efficiency · 18

3.3 Romidepsin improves base editing efficiency at endogenous target sites · · 20

3.4 HDAC inhibitor improves base editing efficiency · · · · · · · · · · · · · · · 22

3.5 Range of base editing window by romidepsin · · · · · · · · · · · · · · · · · 23

3.6 Inhibition of HDAC1 or HDAC2 expression improves ABE−mediated base editing efficiency · 24

3.7 Off−target effect in absence and presence of romidepsin · · · · · · · · · · 25

3.8 Romidepsin increases ABE7.10 protein and gRNA expression level · · · · 26

3.9 Romidepsin increase ABE activity by converting the chromatin state · · · 28

3.10 Romidepsin increase the base editing efficiency of ABEmax and BE4max 30

3.11 Romidepsin increase product purity of base editing · · · · · · · · · · · · 31

4. DISCUSSION · 73

5. REFERENCES · 78

국문요약 · 90

LIST OF FIGURES

Figure 1. Schematic design of HAP1−ABE^{Dox} : EGFP reporter system. · · · · 32

Figure 2. Base editing efficiency of HAP1−ABE^{Dox} cell line. · · · · · · · · · 33

Figure 3. Optimization of the HAP1−ABE^{Dox} : EGFP reporter cell line. · · · · 34

Figure 4. The relative fold−change of EGFP expression level in drug screens. 36

Figure 5. Adenine base editing efficiency at the EGFP target site of HAP1−ABE^{Dox} : EGFP reporter system. · 38

Figure 6. Adenine base editing efficiency at endogenous CCR5 target site. · · 40

Figure 7. Evaluation of cell viability and base editing frequency according to romidepsin concentration. · 42

Figure 8. Romidepsin improves adenine base editing efficiency at endogenous target sites. · 44

Figure 9. Romidepsin improves adenine base editing efficiency in HeLa cells. · 46

Figure 10. HDAC inhibitors improve adenine base editing efficiency. · · · · 47

Figure 11. Effect of base editing window in the absence and presence of romidepsin. · 49

Figure 12. Inhibition of HDAC1 and HDAC2 expression by romidepsin improves adenine base editing efficiency · 51

Figure 13. Analysis of off-target effect by romidepsin · · · · · · · · · · · · 53

Figure 14. Romidepsin enhances adenine base editor protein expression level. 54

Figure 15. Assessment of Cas9- and BE3-mediated mutation frequencies by romidepsin treatment. · 56

Figure 16. Romidepsin enhances alternative promote-driven ABE7.10 expression level. · 58

Figure 17. Romidepsin enhances a U6 promoter-driven gRNA expression level. · 60

Figure 18. Romidepsin improves base editing efficiency by affecting the chromatin state. · 61

Figure 19. The effect of romidepsin in open and closed chromatin region. · · · 63

Figure 20. Romidepsin improves ABEmax- and BE4max-mediated base editing efficiency. · 65

Figure 21. Effect of romidepsin on base editing product purity. · · · · · · · · 67

LIST OF TABLES

Table 1. List of target sequences of gRNA used in the study. · · · · · · · · · · 68

Table 2. List of primer sequences used in the study. · · · · · · · · · · · · · · 69

Table 3. Top 30 drugs in small molecule drug screening. · · · · · · · · · · · 71

Table 4. List of off-target sites. · 72

1. INTRODUCTION

The clustered regularly interspaced short palindromic repeats (CRISPR)-*CRISPR*-associated protein 9 (Cas9) system—first described in nature as an acquired immune system of bacteria or archaea that cleaves foreign bacteriophage DNA sequences— is the most innovative biological tool for gene function research [1, 2]. The principle of the CRISPR-Cas9 system is that when a foreign virus such as a bacteriophage first invades, the bacteria cut the viral DNA into small fragments and insert them into the spacer region located within the CRISPR locus. The CRISPR locus is transcribed to produce mature crRNA and forms a duplex with trans-activating crRNA (tracrRNA) [3]. After this, when the same virus is reinfected, the Cas9 protein and crRNA-tracrRNA duplex form a complex, bind to a complementary sequence to the crRNA within the viral genome and cleave viral DNA [4, 5]. In nature, genetic manipulation is induced by a complex of the Cas9 protein and crRNA-tracrRNA duplex, but it required a simplified composition for efficient use. Therefore, the crRNA and tracrRNA were connected in a loop and engineered into a single structure, and this chimeric gRNA exhibited an activity level like that of the crRNA-tracrRNA duplex [6]. The Cas9 protein and sgRNA form a complex, and recognize the protospacer adjacent motif (PAM) sequence. The PAMs are essential for Cas9 nuclease to cleave DNA and indicate to specific short sequences near target DNA. The most widely used SpCas9, from *streptococcus pyogenes*, recognizes the 5’-NGG-3’ PAM and cleaves the target

sites [7]. Although these Cas9 nucleases have high fidelity by specific PAM sequences, many efforts have been made to relax PAM limitations to expand their targetable sites. Currently, a variety of Cas9 nucleases with individual PAMs from different bacterial species have been discovered, allowing researchers to choose and use Cas9 according to targeting sites [8−10]. More recently, the engineering of Cas9 nuclease has led to the development of variants with less stringent PAM recognition, further expanding the targetable sites [11−13]. After the Cas9:sgRNA complex binds to the target site, Cas9 induces DNA double−strand breaks, which are then repaired by intracellular DNA repair reactions. [14−17] . At the site where DBS occurs, DNA repair factors are recruited to repair DNA. Non−homologous end joining (NHEJ), which occurs mostly, can be used for gene knockout by inducing indels (small insertions or deletions) at the DSB site, and homology−directed repair (HDR) induces to achieve precise genome editing with a homologous donor template [18]. After that, the scope of application was further expanded with the development of various usable Cas9 variants. Cas9 has 2 nuclease domains, the HNH (cleavage of target strand) and RuvC (cleavage of the non−target strand), that cleave the target DNA [19]. The introduction of catalytically inactive mutations in the two nuclease domains, particularly H840A in the HNH domain and D10A in the RuvC domain results in the loss of nuclease activity [3, 6]. Nickase Cas9 (nCas9), which cuts only a single DNA strand by introducing mutations in one domain, can increase specificity and reduce off−targets [20, 21]. dCas9 with mutations in both domains binds to the target site but does not cleave DNA. These

dCas9s can be applied in a variety of technologies by enabling imaging, gene expression control by fusing multiple proteins, and epigenetic studies [22-25].

Recently, CRISPR technology has been applied to various fields such as plant biotechnology, drug discovery, and disease modeling, and is attracting attention as a tool to treat human pathogenic diseases [26-32]. However, since Cas9 nuclease induces DSBs at the target site, it may cause undesirable results, which limits its clinical use. A recent study showed that Cas9-induced DSBs were cytotoxic, and when the mechanism was investigated, it was reported that the p53 gene was activated. The P53 gene is responsible for recognizing DNA damage and preserving genome stability. When DNA is damaged, DNA repair-related factors are recruited, but in case of fatal damage, cell apoptosis is induced. These results can be ineffective and hurdles therapeutic approaches. In addition, cases of causing large chromosomal deletions, genomic rearrangements, and unwanted byproducts or indels by Cas9-mediated DSBs have been reported continuously, which necessitated the development of more effective and precise genome editing tools [33-35]. In addition, more than 60% of mutations associated with pathogenic human disease in ClinVar data are caused by point mutations [36]. Therefore, base editors (BEs) capable of accurate base editing without DNA damage for various SNPs have enormous potential as therapeutic tools. BEs has currently developed two major base editors, the cytosine base editor (CBE) and the adenine base editor (ABE), CBE induces substitutions from C:G to T:A and ABE induces substitutions from A:T to G:C. induce substitution. Initially, CBE was created by fusing rat APOBEC1 to catalytically inactive dCas9 (H840A, D10A) to create BE1 and BE2

with an added uracil glycosylase inhibitor (UGI). This was followed by the development of BE3, which was replaced by nCas9 (D10A) to further improve its efficiency [37]. BE3 nicks at the target DNA strand and converts cytosine to uracil. After this, the DNA repair mechanism forces the guanine in the nicked DNA strand to be repaired to adenine, and finally, the uracil is converted to thymine, resulting in the desired editing result. Afterward, BE4, which was improved by adding more UGIs to BE3, further improved the base editing efficiency [38]. However, most disease-associated mutations are caused by point mutations from G:C to A:T and cannot be corrected by CBE. Therefore, ABEs that induce A:T to G:C mutations have been developed [39]. ABE was constructed using TadA (tRNA-specific adenosine deaminase) from Escherichia coli (E. coli), and TadA has evolved in several steps to operate on DNA. Then, a TadA variant that effectively induces adenine deamination in DNA was discovered, and the definitive version, ABE7.10, was developed by fusing it to nCas9 (D10A). Afterward, CBE and ABE were engineered into BE4max and ABEmax by optimizing codons and tagging nuclear localization sequences (NLS) that are transported to the cell nucleus, which further maximized base editing efficiency [40].

CRISPR-Cas9 technology is widely used, including in human cells and animals, plants, and prokaryotes, but DSB repair-mediated precise editing efficiency varies in many cell types [41-47]. Therefore, further studies were conducted to improve precise genome editing. Previous studies have reported that the use of small-molecule drugs improves the efficiency of Cas9-mediated gene editing. NU7026 and NU7441, which block DNA-PL activity, and SCR7, which suppresses DNA

ligase IV, can improve HDR efficiency by suppressing the NHEJ-mediated repair pathway [48-50]. In addition, RS-1, a RAD51 agonist, can significantly improve HDR efficiency [51, 52]. In addition, inhibition of the ATM and ATR pathways, such as VE-822 and AZD-7762, can enhance the knock-in and knock-in efficiency of CRISPR-Cas12a in human pluripotent cells [53]. In addition, using cell cycle inhibitors such as Aphidicolin and Nocodazole can show cell cycle-dependent gene editing efficiency [54]. Eventually, small molecules with hit productivity, permeability, and low immunity can be an attractive option to improve genome editing efficiency [55, 56]. Although previous studies have shown that small-molecule compounds can improve Cas9-mediated gene editing efficiency, there have been no studies aimed at improving base editing efficiency. Therefore, identifying small molecule drugs to improve CRISPR-based base editing efficiency can be a useful method.

In this study, a fluorescent reporter-based drug screening platform was developed to screen 414 validated small molecule compounds with the potential to improve adenine base editing efficiency. A reporter system with the fluorescence signal turned off is designed so that the fluorescence signal is turned on through the A to G conversion of ABE and gRNA expressed by doxycycline induction. The identified drug in a small molecule drug screen using this reporter system to enhance the fluorescent signal was identified as romidepsin, an HDAC inhibitor. Romidepsin significantly enhanced base editing efficiency at the endogenous target site. The enhanced efficiency of base editing by romidepsin treatment was induced by increased levels of ABE7.10 protein and gRNA expression levels. In addition,

base editing efficiency was significantly increased when RNP was delivered, which excluded expression enhancement by romidepsin treatment. These results showed through the Chip assay that romidepsin inhibits histone deacetylation at the target site and converts the chromatin state to an open state, improving the accessibility of the adenine base editor. In addition, romidepsin increased the expression and mutation frequency of Cas9, BE3 and improved BE (ABEmax and BE4max) as well as ABE7.10. Overall, these results suggest that romidepsin, an HDAC inhibitor, can significantly improve base editing efficiency, which may affect base editing efficiency by enhancing RNP accessibility to open chromatin structures with enhanced expression and suppression of histone acetylation.

2. MATERIALS AND METHODS

2.1 Plasmid DNA preparation

p3s-Cas9HC (Addgene plasmid #43945), pCMV-ABE7.10 (Addgene plasmid #102919) pCMV-BE3 (Addgene plasmid #73021), pCMV-ABEmax (Addgene plasmid #112095), pCMV-BE4max (Addgene plasmid #112093), pCMV-ABEmax-P2A-GFP (Addgene plasmid #112101), and pCMV-BE4max-P2A-GFP (Addgene plasmid #112099) were used in the plasmid DNA transfection. The gRNAs were cloned into a pRG2 plasmid vector (Addgene plasmid #104174), the target sequences are listed in Table 1. To construct reverse plasmid encoding tetracycline-controlled transactivator (rt-TA)-dependent doxycycline-inducible ABE7.10, Cas9 sequences of pCW-Cas9 (Addgene plasmid #50661) were replaced with ABE7.10 of pCMV-ABE7.10 (Addgene plasmid #102919). Then, U6-gRNA and CMV-EGFP were cloned into a lentiviral vector to construct pLX-pLX-⊿EGFP-gRNA containing a stop codon TAG in EGFP for the EGFP reporter system. To prepare the EGFP fusion construct, the P2A-EGFP coding sequence was amplified by Phusion™ High-Fidelity DNA Polymerase and cloned using the Gibson Assembly Master Mix (New England BioLabs) behind the sequences of Cas9, ABE7.10, and BE3. For comparison of expression level according to the promoter, the EFS and hPGK promoter sequences were amplified using Phusion™ High-Fidelity DNA Polymerase and replaced with the CMV of pCMV-ABE7.10-

P2A-EGFP using the e Gibson Assembly Master Mix (New England BioLabs) according to the manufacturer's protocol.

2.2 Cell culture

HEK293T/17 (ATCC CRL-11268) and HeLa (ATCC CCL-2) cells were cultured in Dulbecco's modified Eagles' medium (DMEM) and HAP1 cells were cultured in Iscove's modified Dulbecco's medium (IMDM) supplemented with 10% fetal bovine serum (FBS) and 1% penicillin/streptomycin (Welgene). All Cells were incubated and maintained at 37° C with 5% CO_2.

2.3 HAP1-ABE^{Dox} : EGFP reporter cell line generation

To generation rt-TA dependent HAP1-ABE^{Dox} cell line, 1 X 10^6 HEK293T/17 cells were seeded in a 6-well plate one day before transfection. On the day of transfection, the cells were transfected with pCW-ABE7.10 (2.5 ug), psPAX2 (1.5 ug), and pMD2.G (1 ug) using Lipofectamine 2000 (Thermo Fisher Scientific) according to the manufacturer's protocols and medium was changed after 24h. The supernatant was harvested 48h after transfection and filtered through a 0.45 μm filter to obtain the viral particle. The virus was infected into HAP1 cells with MOI (Multiplicity of infection) = 0.1, selected using puromycin (2 ug/ml) after 24h, and a single colony was isolated as previously described [57]. Briefly, isolated 8 single clones were infected with CCR5 targeting gRNAs, and

adenine base editing frequencies were analyzed by targeted deep sequencing. Among the 8 single clones, the single clone with high base editing frequency (HAP1−ABE^{Dox} #2 clone) were selected and used for further experiments. Then, to generation of HAP1−ABE^{Dox} : EGFP reporter cell line, viral particles were produced in the same method as above using pLX−⊿EGFP−gRNA and infected into a single HAP1−ABE^{dox} #2 clone with MOI=1. The infected cells were selected using blasticidin (BSD) (10 ug/ml) 24h after infection, a fluorescence−based reporter cell line was constructed. To verify the restoration of EGFP signal in the reporter cell line through the expression of ABE7.10 induced by doxycycline, EGFP expression was confirmed using a fluorescence microscope after treatment with doxycycline (0.5 ug/ml), and these cells were used for small molecule drug screening.

2.4 Drug screening

For small molecule drug screening in a fluorescence−based reporter cell line, 2 X 10^4 HAP1−ABE^{Dox} : EGFP reporter cells were seeded in 96−well plates with doxycycline (0.5 ug/ml). 1h after cell seeding, 10 ul of 414 anti−cancer compounds were applied to each well at final concentrations of 100 and 500 nM using a Janus liquid handler (PerkinElmer), referring to the small molecule drug concentrations from manufacturer's guidelines and previous studies [58, 59]. After 48h, the cells were stained using Hoechst33342 dye, and EGFP levels were evaluated using Operetta High Contents Screening system (PerkinElmer). The control set up

wells with DMSO as the negative control and doxycycline as the positive control, hit chemical compounds were selected according to the fold change in EGFP expression level. The Z−prime factor had an average of 0.52 in the 100 nM screen and 0.09 in the 500 nM screen. The all−chemical compounds were evaluated using biological replicates.

2.5 HDAC1 and HDAC2 knockdown cell line generation

To generate HDAC1 and HDAC2 knockdown cell lines, plasmid DNA encoding shRNA targeting HDAC1 and 2 was produced. The target sequence of HDAC1 (TRCN0000195467; 5′ −CGGTTAGGTTGCTTCAATCTA−3′) or HDAC2 (TRCN0000196590; 5′ −GACGGTATCATTCCATAAATA−3′) was cloned into the pLKO_TRC001 (Addgene plasmid #10878) vector and an shRNA−encoding lentivirus was constructed. To produce shRNA−encoding lentivirus, 1 X 10^6 HEK293T/17 cells were seeded in a 6−well plate. When cell confluency reached approximately 80%, the cells were transfected with each sgRNA−expressing vector (2.5 ug), psPAX2 (1.5 ug), and pMD2.G (1 ug) plasmid DNA using Lipofectamine 2000 (Thermo Fisher Scientific) according to manufacturer’s protocol and culture medium was changed after 24h. After 48h of transfection, the lentiviruses were harvested and filtered through a 0.45 μm filter. The harvested lentiviruses were infected into 1 × 10^6 HEK293T/17 cells to generate HDAC1 or HDAC2 knockdown cell lines. After 24h, infected cells were selected puromycin (1 ug/ml), and knockdown of HDAC1 or HDAC2 confirmed

protein expression by the iWestern system (Thermo Fisher Scientific) according to the manufacturer's protocol. Briefly, whole cell lysate (WCL) was loaded in 4–12% Bis–Tris Plus Gel (Thermo Fisher Scientific) and transferred on polyvinylidene difluoride membrane using the iBlot 2 Dry Blotting System. The blotted membrane with anti–HDAC1 (Cell Signaling Technology, #5356), anti–HDAC2 (Cell Signaling Technology, #5113), and anti–glyceraldehyde 3–phosphate dehydrogenase (anti–GAPDH; Santa Cruz Biotechnology, sc–47724) antibodies. The immunoblotted protein bands were detected using enhanced chemiluminescence and quantitated with the ImageJ Gel Analysis program.

2.6 Protein purification

A plasmid encoding the Cas9 and ABE7.10 with His tag was transformed into BL21 Star (DE3)–competent *Escherichia coli* cells and cultured overnight in Luria–Bertani (LB) broth containing kanamycin (50 μg/ml) with shaking at 37° C. 10 ml of overnight cultures were cultured in 400 ml of LB broth containing kanamycin (50 μg/ml) until the optical density at 600 nm (OD_{600}) reached 0.65–0.70 at 37° C. The cells were cooled in Luria–Bertani broth (LB) medium with 1 mM isopropyl β–D–1–thiogalactopyranoside (IPTG) at 18° C for 16 h and harvested by centrifugation at 6000 X g for 10 min at 4° C. The harvested cells were lysed in lysis buffer (50mM NaH_2PO_4, 500 mM NaCl, 10 mM imidazole, 1% Triton X–100, 20% glycerol, 1 mM dithiothreitol [DTT], 1 mM phenylmethylsulphonyl fluoride, 1 mg/ml lysozyme, and 10 μM $ZnCl_2$; pH 8.0) by sonication and the soluble lysates were

obtained using centrifugation at 15000 X g for 20 min. The lysates were applied to Ni-NTA agarose resin (Qiagen), washed, and eluted with a buffer supplemented with 250 mM imidazole. The Cas9 and ABE7.10 proteins were loaded onto a polypropylene column containing heparin agarose beads (GE Healthcare), washed, and eluted with elution buffer (50 mM NaH_2PO_4, 750 mM NaCl, 20% glycerol, 1 mM DTT, 10 μM $ZnCl_2$; pH 8.0). Purified Cas9 and ABE7.10 proteins were diluted with storage buffer (20 mM HEPES, 150 mM KCl, 1 mM DTT, and 10% glycerol; pH 7.5) and concentrated by Amicon ultra-centrifugal filter (Merck).

2.7 Transfection and drug treatment

For plasmid DNA delivery, 1.6 X 10^5 HEK293T/17 cells were seeded in a 24-well plate before 24h of transfection. When cell confluency reached approximately 80%, the cells were transfected with plasmid DNA encoding BEs (ABE7.10, BE3, ABEmax, and BE4max ; 1.5 ug) or Cas9 (0.5 ug) and a plasmid DNA encoding gRNA (0.5 ug) using Lipofectamine 2000 according to the manufacturer' s protocols as previously described [60]. For ribonucleoprotein (RNP) delivery, quantified ABE7.10 protein (10 ug) and synthetic gRNAs (6 ug) were incubated at room temperature for 15 min to assemble the RNP complex. 1.5 X 10^6 HEK293T/17 cells were centrifuged at 100 X g for 10 min at room temperature and washed with DPBS. The washed cells and assembled RNP complex were resuspended in resuspension buffer R and electroporated in two 20-ms pulses of 1300V using Neon transfection system (Thermo Fisher Scientific). 5 nM of romidepsin

(Selleckchem) were treated 6h after plasmid DNA transfection or 1h after RNP electroporation. Genomic DNA was extracted 72h after transfection using the DNeasy Blood & Tissue Kit (Qiagen) according to the manufacturer's protocol.

2.8 Targeted deep sequencing and data analysis

To construct the targeted deep sequencing library, the target region of genomic DNA was amplified with Illumina P5/P7 indexed primer, and the PCR products were amplified with a primer containing sequencing adaptor using Phusion DNA polymerase (New England Biolabs) in third round PCR. The sequencing libraries were subjected to paired-end reads using Illumina Miniseq and joined using the fastq-join tool (https://github.com/brwnj/fastq-join). The base editing frequencies were analyzed using MAUND (https://github.com/ibs-cge/maund) as previously described [60]. The indel and base editing efficiency was also verified using Cas-/BE-Analyzer (http://www.rgenome.net) [61]. The PCR primer sequences used in this study are listed in Table 2.

2.9 Protein expression level measurement

To measure the Cas protein expression level by treatment of small molecule compounds, the following plasmid DNA was delivered. 1.6 X 10^5 HEK293T/17 cells were transfected with 2ug of 2A-EGFP-fused Cas (Cas9, ABE7.10, BE3) plasmid DNA for direct expression level evaluation or 2ug of ABE7.10-P2A-EGFP plasmid

DNA expressed by the three promoters (CMV, EFS, hPGK) to determine the effect of the promoter expressing ABE7.10 using Lipofectamine 2000 and romidepsin (10 nM) was treated 6h after transfection. After 72h of transfection, cells were trypsinized and collected. The EGFP expression levels were measured using a BD FACSCanto Ⅱ and 1 X 10^4 cells were analyzed using Flowjo software. The western blot assay was performed by the iWestern system (Thermo Fisher Scientific) according to the manufacturer's protocol. Western blotting was performed as described above, the blotted membrane with anti-Cas9 (Invitrogen, MA1-201), and anti-glyceraldehyde 3-phosphate dehydrogenase (anti-GAPDH; Santa Cruz Biotechnology, sc-47724) antibodies. The immunoblotted protein bands were detected using enhanced chemiluminescence and quantitated with the ImageJ Gel Analysis program.

2.10 Quantitative PCR

To measure the gRNA expression level by treatment of small molecule drugs, 1.6 X 10^5 HEK293T/17 cells were seeded 24-well plated one day before transfection. When cell confluency was 80%, the cells were transfected with 2 ug plasmid DNA encoding CCR5 and HEK2-targeting gRNAs. To measure the gRNA expression level by treatment of small molecule drugs, the cells were collected after 72h, and total RNA was extracted using a miRNeasy Mini Kit (Qiagen). Then, 1 ug of total RNA was reverse transcribed using miScript II RT Kit (Qiagen) according to the manufacturer's protocol. Quantitative PCR was conducted in triplicates using iQ™

SYBR® Green Supermix (Bio-rad) on a CFX96 Touch Real-Time PCR Detection System (Bio-rad). The gRNA expression levels were normalized to the housekeeping gene (GAPDH) and calculated as the median threshold cycle (Ct) value. Primer sequences used in qPCR are described in Table 2.

2.11 Chromatin immunoprecipitation (ChIP) assay

ChIP assay was performed using a Pierce Magnetic ChIP Kit (Thermo Fisher Scientific) according to the manufacturer's protocol. HEK293T/17 cells were treated with 10 mM romidepsin for 72h and cross-linked with 1% formaldehyde. The cells were lysed and digested by MNase. Then, the lysates were sheared to lengths of 200-1000 bp DNA fragments using three sets of 20-s pulses of sonication. The DNA-protein complexes were precipitated using anti-normal rabbit IgG included in the kit or anti-acetyl-histone H3 Lys9 antibody (Upstate Biotechnology). The immunoprecipitated DNA was measured using qPCR. The primer sequences in the used ChIP assay are described in Table 2.

3. RESULTS

3.1 Generation of HAP1−ABE^{Dox} : EGFP cell line

To identify novel small molecules that improve ABE efficiency, a fluorescence-based reporter system that can be applied for drug screening was developed (Figure. 1). To construct a fluorescent reporter cell line, HAP1 cells were sequentially infected with the 2 cassettes. First, the rt-TA-dependent HAP1-ABE^{Dox} cell line was generated, and a single clone was isolated. For the clonal assay, eight HAP1-ABE^{Dox} single clones were delivered with lentiviral CCR5 targeting gRNA, and ABE expression was induced by treatment with doxycycline (2 ug/ml) after 6h (Figure. 2). 72h after infection, genomic DNA was extracted, and adenine base editing efficiency was analyzed by targeted deep sequencing. Clone #2 showed the highest base editing efficiency and was selected for further investigation. Then, clone #2 was integrated with a cassette containing the EGFP targeting gRNA and the EGFP encoding sequence. In the EGFP sequence, an artificial premature stop codon is inserted behind the start codon so that EGFP is not expressed. When ABE7.10 expression is induced by doxycycline treatment, ABE7.10 protein, and EGFP targeting gRNAs converted the stop codon to glutamine (TAG to CAG). and the EGFP protein expression was restored. For drug screening, the percentage of GFP expression restoration was evaluated at different cell densities and doxycycline concentrations to determine optimal conditions. The

HAP1−ABE^{Dox} : EGFP reporter cell line showed EGFP expression levels dependent on cell density and doxycycline concentration (Figure. 3 A). The 2 X 10^4 cells/ml density and 2 ug/ml of doxycycline were selected to calculate EGFP fluorescence signal changes caused by candidate in subsequent small molecule drug screening. Under the selected optimal conditions, EGFP−positive cells were observed using a fluorescence microscope (Figure. 3 B). Therefore, these results indicate that the fluorescence−based reporter system is successfully constructed.

3.2 Small molecule drug screening to improve adenine base editing efficiency

A validated 414 anti-cancer drug library with the potential to improve ABE efficiency was screened using the EGFP reporter system. For initial screening, all small molecule compounds were treated at two concentrations (100 or 500 mM) for 48h, and EGFP expression levels were measured with the high-throughput system. The fold-change in EGFP expression level of small molecule compounds-treated cells was calculated by normalizing the level of cells treated with doxycycline alone (Figure. 4). As a result, romidepsin, which is the HDAC inhibitor, showed the largest change on the fold-change of EGFP expression levels with 5.33-fold change at 100 nM and 7.79-fold change at 500 nM. In addition, HDAC inhibitors such as quisinostat, trichostatin A (TSA), and abexinostat were ranked at the top in both concentration conditions. The top 30 small molecule compounds in the drug screen are listed in Table 3. Therefore, through these results, it was investigated whether HDAC inhibitor improves the adenine base editing efficiency.

To confirm that EGFP protein expression was restored by ABE7.10-mediated A to G conversion, romidepsin-treated cells with the highest rank were analyzed for EGFP target sites by targeted deep sequencing (Figure. 5). The A to G conversion frequency at position 6 in the editing window was 37.9% when only doxycycline was treated, but significantly improved to 72.9% when doxycycline and romidepsin were treated together. Therefore, these results indicate that HDAC inhibitors, including romidepsin, significantly increase the expression level of EGFP in the

HAP1-ABE^{Dox} : EGFP reporter system and that EGFP is restored by A to G conversion at the EGFP target site.

3.3 Romidepsin improves base editing efficiency at endogenous target sites

The romidepsin was evaluated to affect ABE efficiency at endogenous target sites. First, HEK293T/17 cells were transfected with plasmid DNA ABE7.10 and CCR5 targeting gRNAs and treated with 10 nM of romidepsin after 6h. After 72h of transfection, genomic DNA was extracted from the cells, and base editing efficiency was analyzed using targeted deep sequencing (Figure. 6). At position 5 located in the canonical editing window of ABE7.10, the A to G editing efficiency increased 3.5-fold from 10.7% (non-treat) to 37.9% with romidepsin treatment. Then, the romidepsin concentration was optimized to exclude drug toxicity. Naïve HEK293T/17 cells were treated with 2 - 100 nM of romidepsin for 72h, and the number of cells was counted to evaluate cell viability (Figure. 7 A). Compared to cells not treated with romidepsin (Mock), dose-dependent cell viability was confirmed. In addition, to evaluate the ABE efficiency according to the romidepsin concentration, HEK293T/17 cells were delivered ABE7.10 and gRNA targeting 4 endogenous target sit, treated with 2-100 nM of romidepsin (Figure. 7 B). The 5 nM of romidepsin was most effective in improving ABE efficiency, and the romidepsin concentration was determined for the subsequent experiments. Then, ABE efficiency by romidepsin treatment was evaluated at 16 endogenous target sites (Figure. 8 A). The romidepsin improved ABE efficiency, especially at the ZNF195 site, from 2.18% to 8.32%, up to 3.8-fold. Statistically, romidepsin improved the ABE efficiency more than 1.68-fold (Figure. 8 B). Then, the effect of romidepsin was evaluated in HeLa cells. At the 4 endogenous target sites in HeLa cells, the romidepsin improved adenine base editing efficiency, especially at TYRO3

site by up to 4.6−fold (Figure. 9). Therefore, these results indicate that romidepsin can enhance ABE efficiency at the endogenous target sites and has significant effects in other cell types, not limited to HEK293T/17 cells.

3.4 HDAC inhibitor improves base editing efficiency

Next, 4 HDAC inhibitors, including romidepsin, were ranked in the top 30 drugs in a drug screen. Therefore, the effect of the other 3 HDAC inhibitors, abexinostat, quisinostat, and TSA, on base editing efficiency was also evaluated. Three drugs significantly improved the base editing efficiency at the endogenous target sites. (Figure. 10 A). Interestingly, vorinostat, another HDAC inhibitor included in the drug library, was not ranked as the candidate in the drug screening. Vorinostat operates at concentrations 10 to 100−fold higher than those used in drug screening. Therefore, 0.5 uM of vorinostat has been shown to improve adenine base editing efficiency (Figure. 10 B). These results indicate that HDAC inhibitors can improve base editing efficiency at endogenous target sites.

3.5 Range of base editing window by romidepsin

Canonical editing windows of ABE are A4 to A8 in protospacer counting from PAM (counting as 21 to 23 at PAM sequence). However, as shown in Figure 6, the treatment of romidepsin increased the base editing efficiency at the A8 and A9 positions outside the base editing window. Therefore, to confirm the expansion of base editing window by romidepsin treatment, the fold-change of base editing efficiencies was observed for all adenines in the protospacer sequence at 16 endogenous target sites. Romidepsin did not affect the range of the base editing window (Figure 11 A). In addition, different amounts of ABE7.10 were transfected, and the range of the base editing window was analyzed in the absence and presence of romidepsin (Figure 11 B). There was no difference in the range of the base editing window in the two samples transfected with 300 ng and 75 ng of ABE7.10, which showed similar base editing efficiency. Therefore, these results indicate that the improvement of base editing efficiency by romidepsin does not affect the expansion of the editing window.

3.6 Inhibition of HDAC1 or HDAC2 expression improves ABE-mediated base editing efficiency

The HDAC inhibitors, such as romidepsin, TSA, abexinostat, and quisinostat, which are ranked top through drug screening results, are well known to inhibit both HDAC1 and HDAC2. Therefore, to confirm the effect of inhibiting HDAC1 and HDAC2 expression on ABE activity, HDAC1 or HDAC2 knockdown HEK293T/17 cell lines were generated using shRNA (Figure. 12 A). In cells in which HDAC1 or HDAC2 expression level was downregulated, ABE7.10 and gRNA targeting 3 endogenous sites were transfected and targeted deep sequencing was performed after 72h. It significantly increased ABE efficiency at evaluating all target sites (Figure. 12 B), indicating that HDAC inhibitors may contribute to the enhancement of ABE efficiency by inhibiting HDAC1 or HDAC2 expression.

3.7 Off-target effect in the absence and presence of romidepsin

The off-target effects of romidepsin were investigated at Tyro3 and HEK2 sites, which were previously identified as having off-target sites (Figure. 13). The HEK293T/17 cells were transfected with ABE7.10 and TYRO3 or HEK2 targeting gRNA plasmid DNA, sequenced at on-target and off-target sites. The off-target site sequences are listed in Table 4. The romidepsin, an HDAC inhibitor, enhanced the ABE efficiency at both on- and off-target activity.

3.8 Romidepsin increases ABE7.10 protein and gRNA expression level

The HDAC inhibitors are known to enhance the expression of plasmid DNA into mammalian cells and the CMV promoter-driven gene expression [62-64]. Increased ABE protein expression contributed significantly to ABE activity, so ABE expression change by HDAC inhibitor was measured. To measure ABE protein expression, ABE7.10-2A-EGFP plasmid DNA, in which 2A-EGFP was fused to the behind of the ABE sequence, was constructed (Figure 14 A), and transected into HEK293T/17 cells. Romidepsin was treated 6h after transfection, and the percentage of GFP-positive cells was measured using flow cytometry after 72h. The GFP-positive cells increased 3.6-fold (13.4% →48.2%) (Figure. 14 B), and the increase in ABE protein expression was verified through western blot assay (Figure. 14 C). The expression levels of Cas9 and BE3 by romidepsin were also significantly increased by 1.2-fold and 4.7-fold, respectively. In addition, to evaluate the improvement of Cas9 and BE3-mediated gene editing efficiency by romidepsin, genome editing efficiency was analyzed at various endogenous target sites (Figure. 15 A, B). The Cas9-mediated indels and BE3-mediated C to T conversion frequencies were increased up to 1.8-fold and 4.4-fold.

Next, the CMV promoter of the ABE7.10 construct was replaced with the EF-1α short (EFS) and human phosphoglycerate kinase (hPGK) to evaluate the alternative promoter-derived ABE7.10 expression of romidepsin (Figure 16 A). The romidepsin increased GFP expression level by EFS and hPGK promoter as well as CMV promoter (Figure. 16 B). This protein expression enhancement also improved

the ABE efficiency at 2 endogenous target sites, such as CCR5 and RNF2 (Figure. 16 C). In addition, romidepsin was predicted to enhance base editing efficiency by increasing the expression level of U6 promoter-driven gRNA. The HEK293T/17 cells were transfected with gRNA plasmid and treated with 10 nM romidepsin after 6h. After 72h of transfection, gRNA expression levels were detected using qPCR. It was confirmed that romidepsin increased relative gRNA expression as previously described, and HDCA inhibitors enhance RNP polymerase III promoter-driven small RNA [65] (Figure. 17). These findings demonstrate that romidepsin improves ABE editing activity by enhancing ABE protein and gRNA expression.

3.9 Romidepsin increases ABE activity by converting the chromatin state.

Previous studies have reported that compact chromatin and nucleosomes in eukaryotes affect indel induction by interfering with Cas9 protein access [66–70]. The HDAC inhibitor, identified in drug screening, can induce chromatin into an open state through histone hyperacetylation. It was anticipated that HDAC inhibitors would increase ABE7.10 protein accessibility by inhibiting histone deacetylation, thereby improving ABE efficiency. To exclude the effect of protein expression by romidepsin, HEK293T/17 cells were electroporated with ABE7.10 ribonucleoprotein (RNP) complexed with quantified ABE7.10 protein and gRNA are complexed and treated with 10nM romidepsin after 6h. (Figure. 18 A) The base editing efficiencies were increased up to 4.9–fold (6.9–34.2% at ABE site 2) in all 4 endogenous target sites. Then, as described above, whether the improvement of base editing efficiency is affected by the chromatin state was investigated through ChIP assay (Figure. 18 B). ChIP assay was performed at 4 endogenous target sites using an antibody against histone H3 acetylation. Romidepsin was shown to increase H3 acetylation at all target sites. These results demonstrate that romidepsin converts chromatin to an open state by inhibiting histone acetylation, which enhances the accessibility of ABE7.10 RNPs at the target site and increases base editing efficiency. In addition, to determine whether the BE–mediated base editing efficiency is affected by the intracellular chromatin state, the effect of romidepsin on open and closed chromatin regions was investigated. In a previous study, the identical DNA sequence present in both open and closed chromatin regions was selected to study Cas9 activity according to the chromatin state, and

the effect of romidepsin was analyzed in these target sequences (Figure 19 A). Therefore, referring to the target sites analyzed in DIG-seq, four target sites were evaluated for the ABE and CBE efficiencies according to the chromatin state. ABE significantly improved the efficiency of base editing by romidepsin in the closed chromatin region than in the open chromatin region (Figure 19 B). However, CBE improved the efficiency of base editing by romidepsin in both open and closed chromatin regions (Figure 19 C). These results suggest that the chromatin state may affect the efficiency of base editors, but other unknown factors may also intervene.

3.10 Romidepsin increases the base editing efficiency of ABEmax and BE4max

ABEmax and BE4man with optimized codon and NLS sequences significantly improved the base editing efficiency [40], and it was investigated whether romidepsin further improves the efficiency of the improved BE variants. To evaluate the protein expression enhancement, an ABEmax/BE4max-2A-EGFP plasmid was constructed fusing 2A-EGFP behind of ABEmax and BE4max sequences (Figure 20 A). After transfection of each plasmid DNA, cells were maintained for 72h with 10 nM romidepsin. GFP expression levels increased from 32.1% to 51.9% in ABEmax and from 34.7% to 54.7% in BE4max (Figure. 20 B), and both BE variants improved base editing efficiency up to 4.8-fold (4.8 % → 20.4 % at the ZNF195 site) at 4 endogenous target sites (Figure. 20 C, D). These results indicated that romidepsin improves the base editing efficiency of enhanced ABEmax and BE4max.

3.11 Romidepsin increases product purity of base editing

The product purity of base editors is affected by DNA repair mechanisms. HDCA inhibitor, as a regulator of DNA damage response, was expected to affect the product purity of CRISPR-mediated base editing [71]. In previous studies, ABE induces A to G conversion with high product purity [39]. As expected, romidepsin improved adenine base editing efficiency but did not affect product purity. To confirm that romidepsin improves CBE product purity, HEK2 and CCR5 sites with low CBE product purity were evaluated [38]. Romidepsin significantly improved C to T editing purity at 2 target sites (Figure. 21 A, B). Consequently, these results indicate that romidepsin can improve the product purity of CBE-mediated base editing.

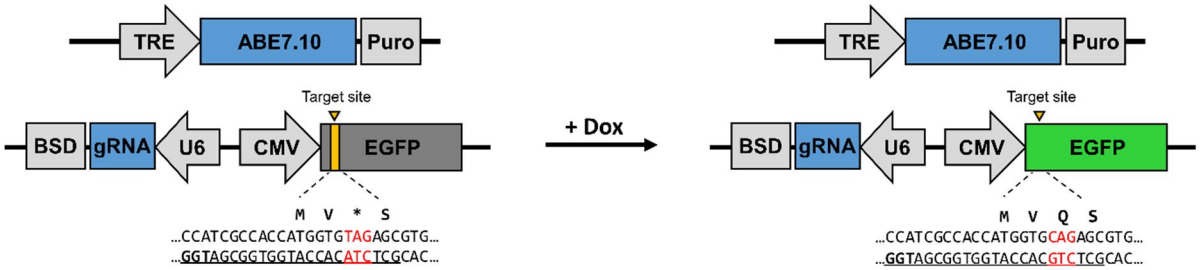

Figure 1. Schematic design of HAP1−ABE^{Dox} : EGFP reporter system.

To generate the reporter cell line, two constructs were designed and subsequently integrated into the HPA1 cell line. HAP1 cell lines were infected with a doxycycline−inducible ABE7.10 expression cassette to generate the HAP1−ABE^{Dox} cell line. Then, a cassette encoding CMV promoter−driven EGFP including a premature stop codon, and U6 promoter−driven EGFP−targeting gRNA was integrated HAP1−ABE^{Dox} cell line. In HAP1−ABE^{Dox} : GFP reporter cell lines, when ABE is expressed by doxycycline, the EGFP−targeting gRNA can convert the stop codon to glutamine to detect fluorescence signals.

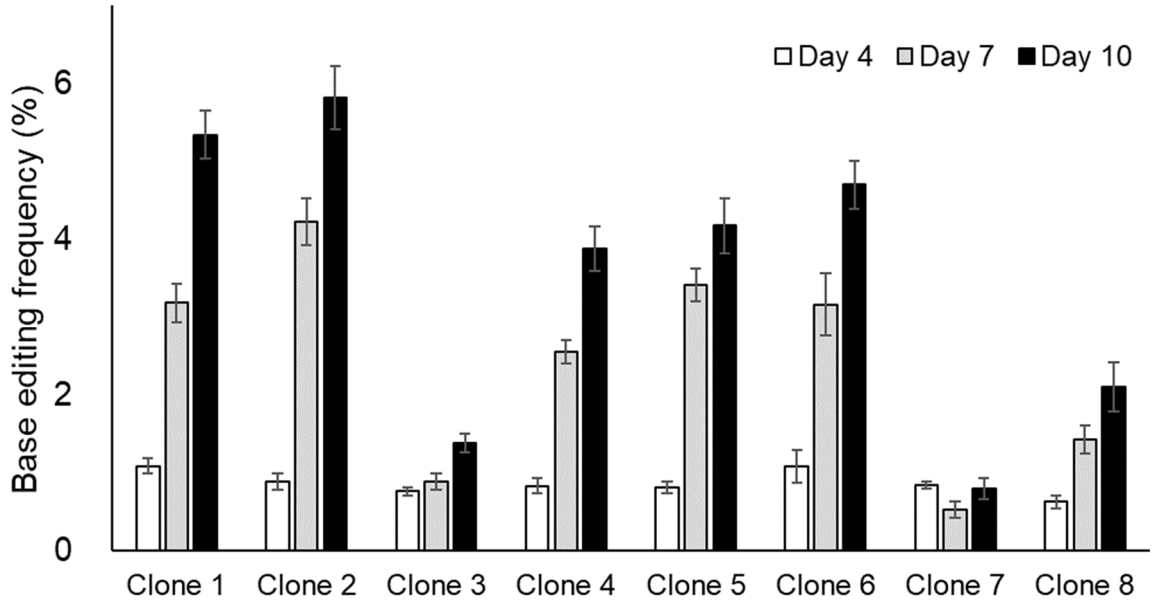

Figure 2. Base editing efficiency of HAP1−ABE^{Dox} cell line

To identify the single clone with the highest ABE activity, 8 HAP1−ABE^{Dox} single clone was infected with a lentivirus containing the CCR5−targeting gRNA. For ABE expression, doxycycline (2 ug/ml) was treated, and adenine base editing efficiency was evaluated by targeted deep sequencing. Clone #2 having the highest base editing efficiency was selected for the generation of the fluorescent−based reporter cell line. Error bars indicate s.e.m. (n = 2).

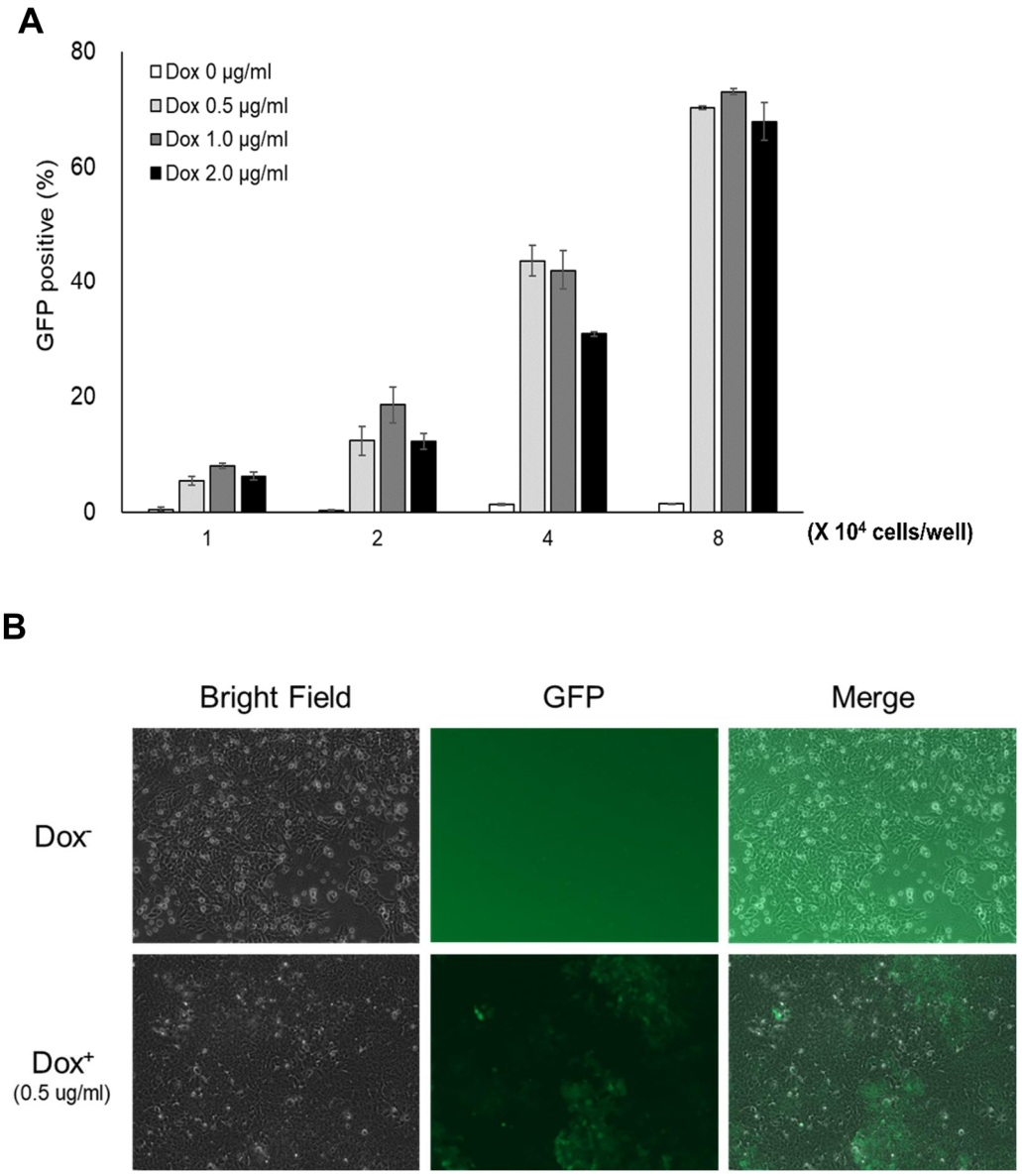

Figure 3. Optimization of the HAP1−ABE^{Dox} : EGFP reporter cell line.

(A) For drug screening, appropriate cell density and doxycycline concertation were evaluated. In a 96−well scale, EGFP expression levels were analyzed using flow cytometry after 48h of doxycycline treatment. Error bars indicate s.e.m. (n = 2). (B) GFP expression restoration by doxycycline in HAP1−ABE^{Dox} : EGFP cell line. The HAP1−ABE^{Dox} : EGFP cell line was restored by doxycycline (0.2 ug/ml)

treatment and EGFP-positive cells were detected under the bright, fluorescence emission, merge field using a fluorescence microscope.

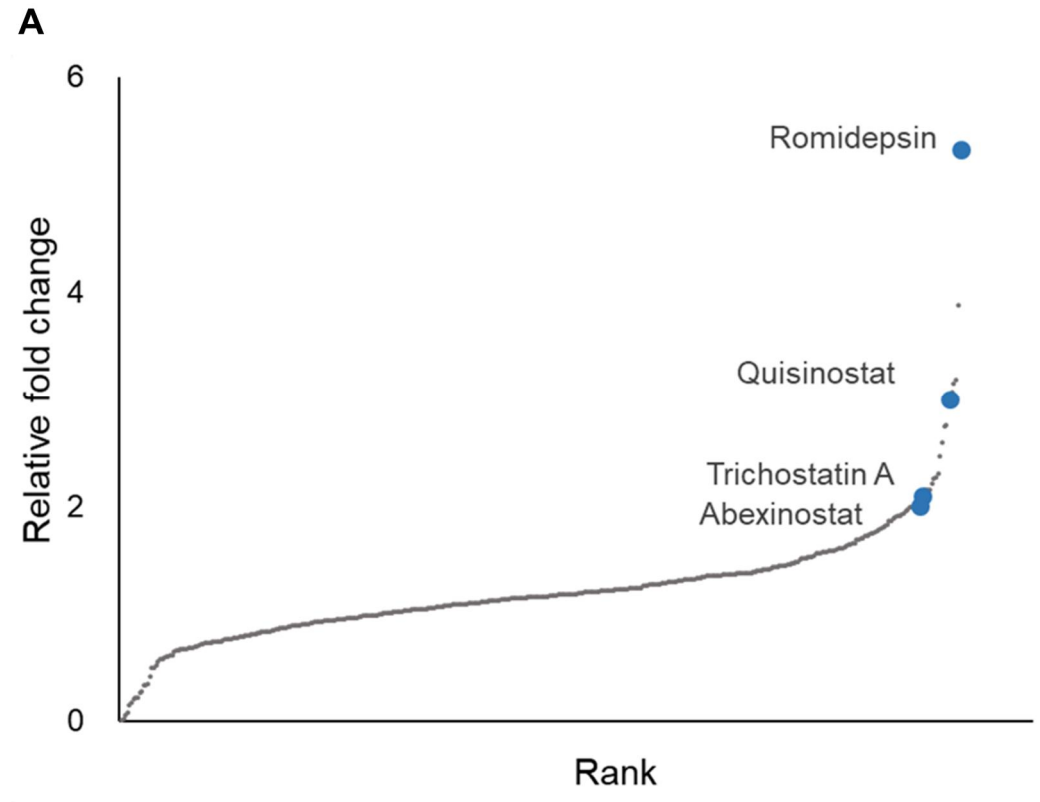
A
6
4
2
0
Relative fold change
Romidepsin
Quisinostat
Trichostatin A
Abexinostat
Rank

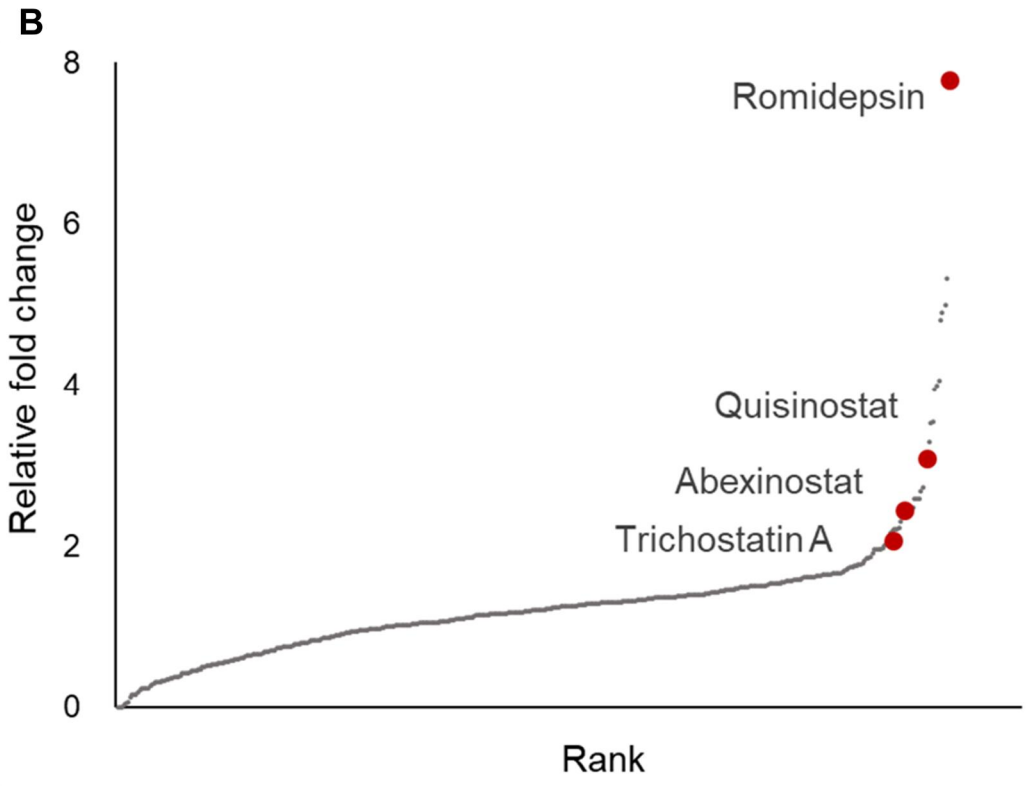
B
8
6
4
2
0
Relative fold change
Romidepsin
Quisinostat
Abexinostat
Trichostatin A
Rank

Figure 4. The relative fold-change of EGFP expression level in drug screens.

414 small molecule compounds with anti-cancer properties were screened at concentrations of (A) 100 nM and (B) 500 nM. The EGFP expression level of each drug-treated cell was calculated as a fold-change relative to the EGFP expression level of cells treated with doxycycline alone. 4 HDAC inhibitors are indicated, respectively. The raw numbers are listed in Table 3 and all small molecule compounds were evaluated using biological replicates.

Untreated

	G_1	C_2	T_3	C_4	T_5	A_6	C_7	A_8	C_9	C_{10}	A_{11}	T_{12}	G_{13}	G_{14}	T_{15}	G_{16}	G_{17}	C_{18}	G_{19}	A_{20}	T_{21}	G_{22}	G_{23}	Indel%
A	0.1	0.0	0.1	0.0	0.1	99.3	0.0	99.2	0.0	0.0	99.7	0.0	0.1	0.1	0.1	0.1	0.1	0.0	0.1	99.5	0.0	0.1	0.1	0.2
C	0.0	99.7	0.5	99.8	0.2	0.4	99.9	0.0	99.9	99.8	0.0	0.4	0.0	0.0	0.2	0.0	0.0	99.6	0.0	0.0	0.4	0.0	0.0	
G	99.9	0.2	0.0	0.1	0.0	0.3	0.0	0.8	0.0	0.0	0.3	0.1	99.9	99.9	0.0	99.9	99.9	0.1	99.8	0.5	0.1	99.9	99.8	
T	0.0	0.1	99.5	0.1	99.7	0.0	0.1	0.0	0.1	0.1	0.0	99.4	0.0	0.0	99.7	0.0	0.0	0.2	0.0	0.0	99.5	0.0	0.0	

Dox+

	G_1	C_2	T_3	C_4	T_5	A_6	C_7	A_8	C_9	C_{10}	A_{11}	T_{12}	G_{13}	G_{14}	T_{15}	G_{16}	G_{17}	C_{18}	G_{19}	A_{20}	T_{21}	G_{22}	G_{23}	Indel%
A	0.1	0.0	0.0	0.0	0.1	61.5	0.0	98.1	0.0	0.1	99.5	0.0	0.1	0.1	0.0	0.1	0.1	0.0	0.1	99.7	0.1	0.1	0.1	0
C	0.0	99.7	0.3	99.8	0.2	0.6	99.8	0.0	99.8	99.9	0.0	0.2	0.0	0.0	0.2	0.0	0.0	99.8	0.0	0.0	0.3	0.0	0.0	
G	99.9	0.2	0.0	0.1	0.0	37.9	0.0	1.8	0.0	0.0	0.5	0.1	99.9	99.8	0.0	99.9	99.8	0.0	99.9	0.3	0.0	99.8	99.8	
T	0.0	0.1	99.7	0.1	99.7	0.0	0.2	0.0	0.1	0.1	0.0	99.6	0.0	0.0	99.8	0.0	0.1	0.2	0.0	0.0	99.7	0.0	0.1	

Dox+ Romidepsin +

	G_1	C_2	T_3	C_4	T_5	A_6	C_7	A_8	C_9	C_{10}	A_{11}	T_{12}	G_{13}	G_{14}	T_{15}	G_{16}	G_{17}	C_{18}	G_{19}	A_{20}	T_{21}	G_{22}	G_{23}	Indel%
A	0.1	0.1	0.0	0.0	0.1	26.4	0.0	96.5	0.0	0.0	99.1	0.0	0.1	0.1	0.1	0.1	0.1	0.0	0.1	99.7	0.0	0.1	0.1	1.8
C	0.0	99.6	0.4	99.6	0.4	0.7	99.8	0.0	99.8	99.9	0.0	0.2	0.0	0.1	0.2	0.0	0.0	99.7	0.0	0.0	0.3	0.0	0.0	
G	99.8	0.2	0.0	0.3	0.0	72.9	0.0	3.4	0.0	0.0	0.9	0.0	99.9	99.9	0.0	99.9	99.9	0.1	99.8	0.3	0.1	99.9	99.8	
T	0.0	0.2	99.6	0.1	99.5	0.0	0.2	0.1	0.2	0.1	0.0	99.7	0.0	0.0	99.7	0.0	0.1	0.2	0.0	0.0	99.6	0.0	0.0	

Figure 5. Adenine base editing efficiency at the EGFP target site of HAP1−ABE^{Dox} : EGFP reporter system

In the target base position, A6, doxycycline alone treatment has a 37.9% A to G conversion frequency: however, when combined with 10 nM of romidepsin, conversion frequency increases up to 72.9%.

Romidepsin -

	T_1	G_2	A_3	C_4	A_5	T_6	C_7	A_8	A_9	T_{10}	T_{11}	A_{12}	T_{13}	T_{14}	A_{15}	T_{16}	A_{17}	C_{18}	A_{19}	T_{20}	**C_{21}**	**G_{22}**	**G_{23}**	Indel%
A	0.0	0.0	98.8	0.0	89.2	0.0	0.0	98.7	99.5	0.0	0.0	99.8	0.0	0.0	99.9	0.0	99.9	0.0	99.8	0.0	0.0	0.1	0.2	0.02
C	0.3	0.0	0.0	99.8	0.1	0.4	99.9	0.1	0.0	0.1	0.1	0.1	0.0	0.2	0.0	0.2	0.0	99.9	0.1	0.3	99.6	0.0	0.0	
G	0.1	100	1.2	0.0	10.7	0.0	0.0	1.2	0.4	0.0	0.0	0.2	0.0	0.0	0.1	0.0	0.1	0.0	0.1	0.1	0.0	99.9	99.7	
T	99.6	0.0	0.1	0.1	0.1	99.6	0.1	0.0	0.0	99.9	99.9	0.0	99.9	99.8	0.0	99.8	0.0	0.1	0.0	99.6	0.4	0.1	0.0	

Romidepsin +

	T_1	G_2	A_3	C_4	A_5	T_6	C_7	A_8	A_9	T_{10}	T_{11}	A_{12}	T_{13}	T_{14}	A_{15}	T_{16}	A_{17}	C_{18}	A_{19}	T_{20}	**C_{21}**	**G_{22}**	**G_{23}**	Indel%
A	0.0	0.0	97.1	0.0	62.1	0.0	0.0	89.3	94.5	0.0	0.0	97.3	0.0	0.0	99.8	0.0	99.7	0.0	99.8	0.0	0.1	0.1	0.0	0
C	0.3	0.0	0.0	99.9	0.1	0.6	100	0.0	0.0	0.1	0.1	0.0	0.2	0.2	0.0	0.2	0.0	100	0.0	0.3	99.9	0.0	0.0	
G	0.0	100	2.9	0.0	37.9	0.0	0.0	10.6	5.5	0.0	0.0	2.7	0.0	0.0	0.2	0.0	0.3	0.0	0.2	0.0	0.0	99.9	99.9	
T	99.7	0.0	0.1	0.1	0.1	99.3	0.0	0.0	0.0	99.9	99.9	0.0	99.8	99.8	0.0	99.8	0.0	0.0	0.0	99.7	0.1	0.0	0.0	

Figure 6. Adenine base editing efficiency at endogenous CCR5 target site.

HEK293T/17 cells were transfected with ABE7.10 and CCR5 targeting gRNA, and 10 nM of romidepsin was treated after 6h. Base editing efficiency was analyzed using targeted deep sequencing. In the target base position, A5, romidepsin treatment improved the A to G conversion frequency from 10.7 % to 37.9 %.

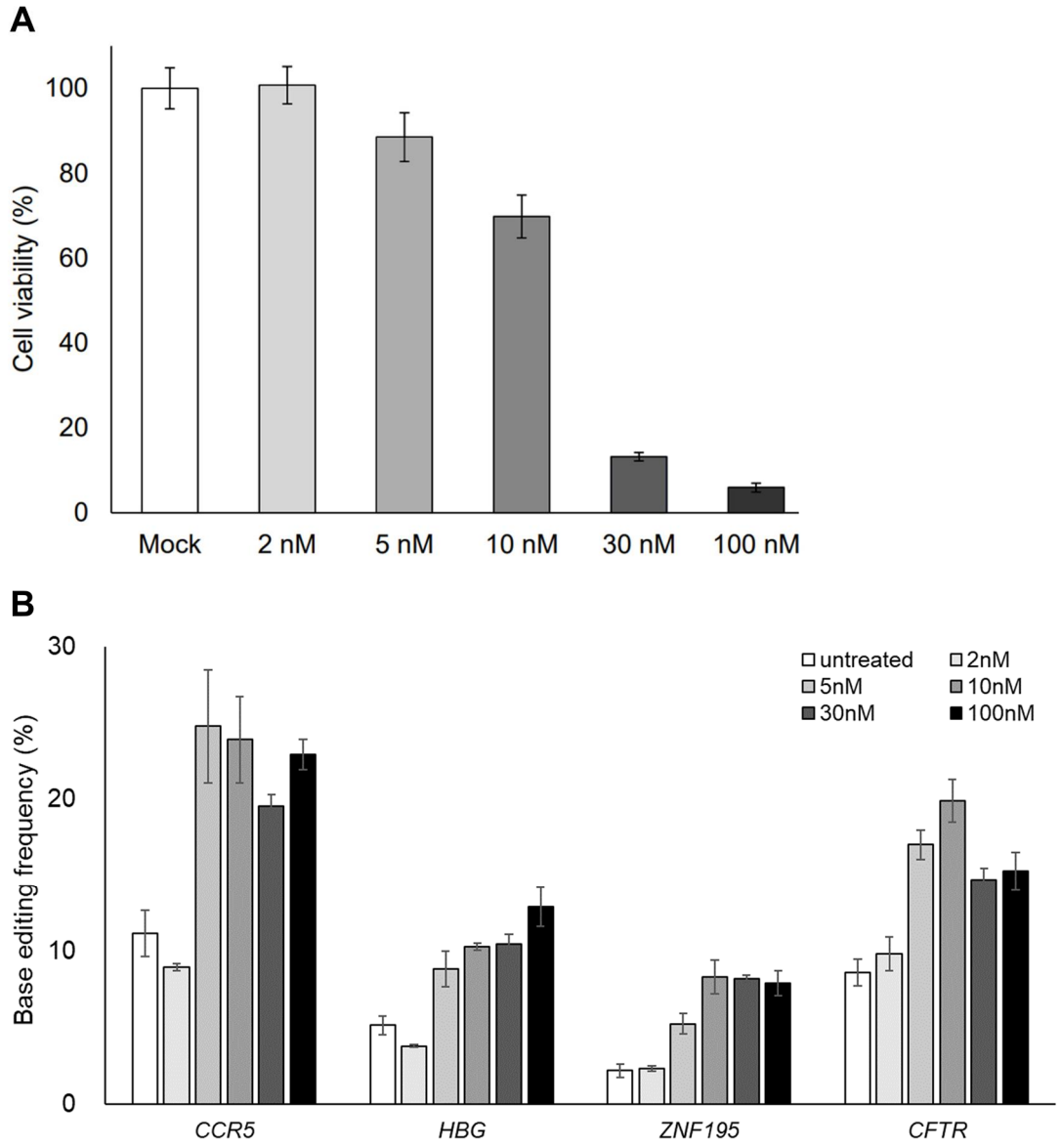

Figure 7. Evaluation of toxicity and base editing frequency according to romidepsin concentration

Analysis of base editing efficiency based on romidepsin concentration at endogenous target sites. HEK293T/17 cells were transfected with ABE7.10 and gRNA plasmid DNA, and romidepsin of the designed concentration was treated after 6h. After 72h

of transfection, base editing frequency was analyzed using targeted deep sequencing. The error bars indicate s.e.m. (n = 3).

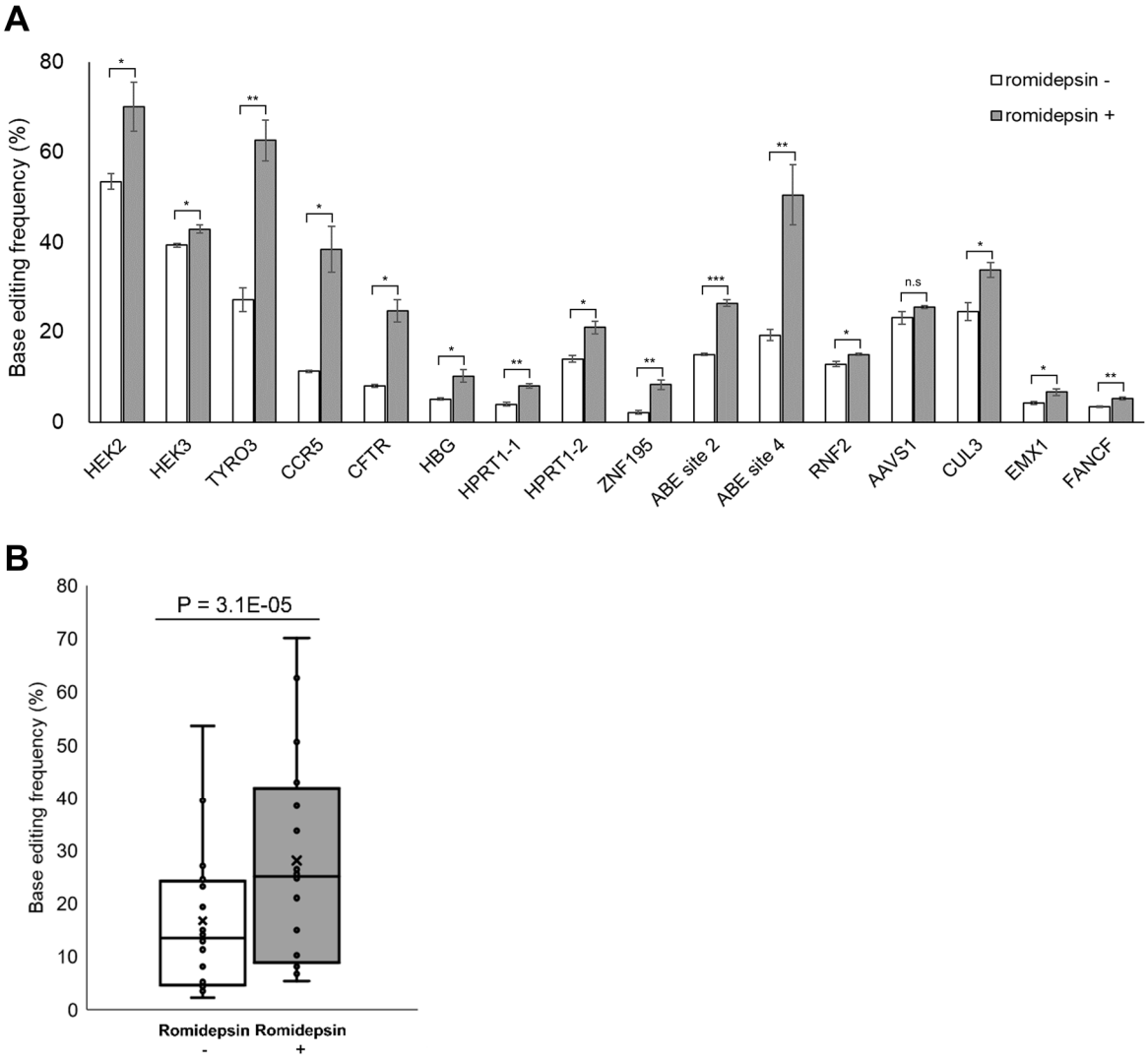

Figure 8. Romidepsin improves adenine base editing efficiency at endogenous target sites.

(A) The enhancement of base editing efficiency by romidepsin at 16 endogenous target sites was evaluated. In almost endogenous target sites, romidepsin improved the adenine base editing efficiency (B) cumulative base editing efficiency across the all-target sites. The two-tailed Wilcoxon signed-rank test was utilized to determine the P-value in the boxplot. Error bars indicate s.e.m (n = 3). Ns, not

significant; $P \geq 0.05$; $*P < 0.05$; $**P < 0.01$; $***P < 0.001$; $****P < 0.0001$ (using two−tailed Student's t−test).

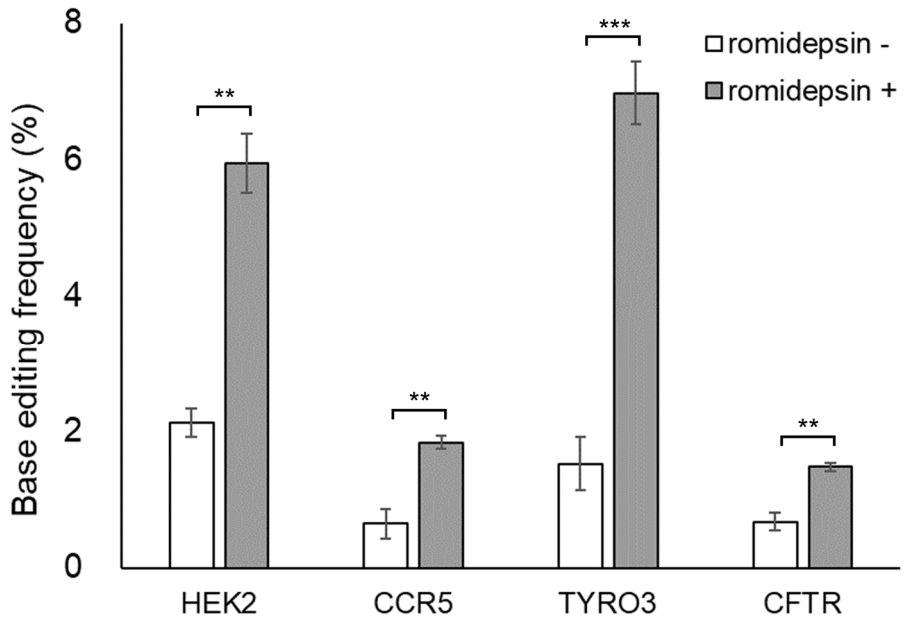

Figure 9. Romidepsin improves adenine base editing efficiency in HeLa cell

Romidepsin increases adenine base editing efficiency at 4 endogenous target sites in HeLa cells. Error bars indicate s.e.m. (n = 3); **P < 0.01; ***P < 0.001 (using two-tailed Student's t-test).

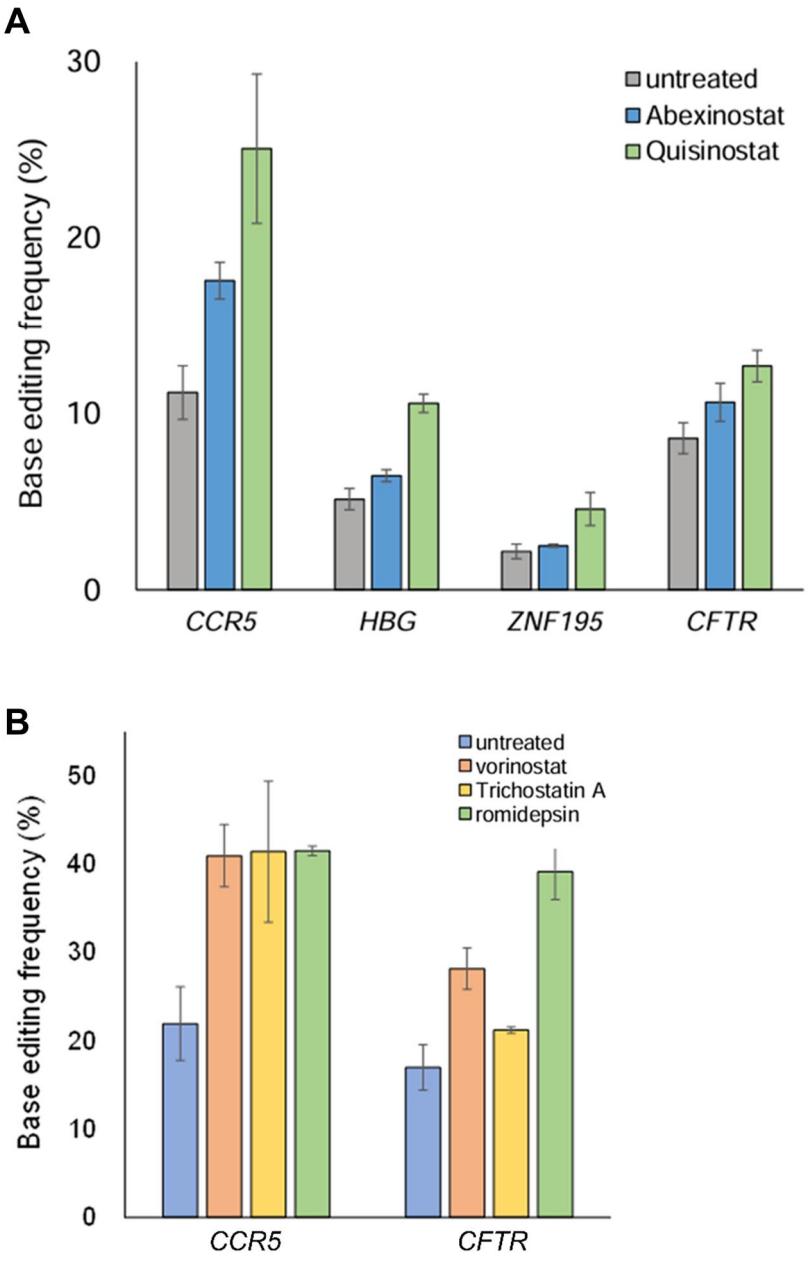

Figure 10. HDAC inhibitors improve adenine base editing efficiency.

HEK293T/17 cells were transfected with ABE7.10 and gRNA targeting each four endogenous target sites. Transfected cells were incubated with abexinostat (5 nM)

or quisinostat (5 nM) (A) vorinostat (0.5 uM), trichostatin A (100 nM), or romidepsin (10 nM) (B). Error bars indicate s.e.m. (n=3).

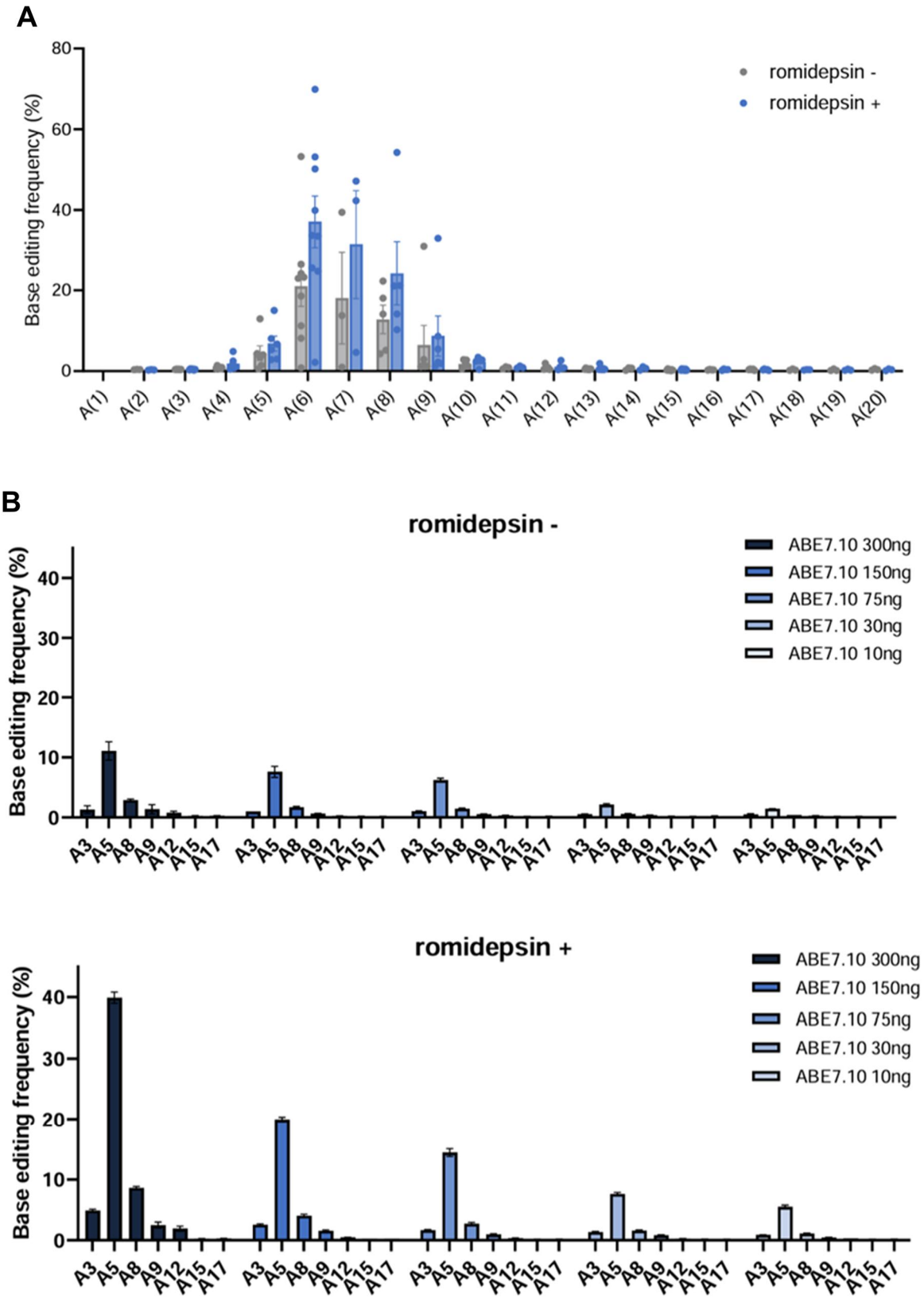
A
Base editing frequency (%)
romidepsin -
romidepsin +
A(1)
A(2)
A(3)
A(4)
A(5)
A(6)
A(7)
A(8)
A(9)
A(10)
A(11)
A(12)
A(13)
A(14)
A(15)
A(16)
A(17)
A(18)
A(19)
A(20)
B
romidepsin -
ABE7.10 300ng
ABE7.10 150ng
ABE7.10 75ng
ABE7.10 30ng
ABE7.10 10ng
Base editing frequency (%)
romidepsin +
ABE7.10 300ng
ABE7.10 150ng
ABE7.10 75ng
ABE7.10 30ng
ABE7.10 10ng
Base editing frequency (%)

Figure 11. Effect of base editing window in the absence and presence of romidepsin

(A) To analyze changes in the extent of the base editing window in the absence and presence of romidepsin, A to G conversion efficiency was confirmed for all adenines in the 16 endogenous target sites used in this study. (B) Analysis of the base editing window according to different amounts of ABE7.19 in the absence and presence of romidepsin. In a 96well scale, HEK293T/17 cells were transfected with different amounts of plasmid DNA (300, 150, 75, 30, 10 ng of ABE7.10 containing 100, 100, 75, 30, 10 ng of CCR5 targeting gRNA) and treated 10 nM of romidepsin after 6h. 72h after transfection, gDNA was extracted and analyzed by targeted deep sequencing. Error bars indicate s.e.m. (n=3)

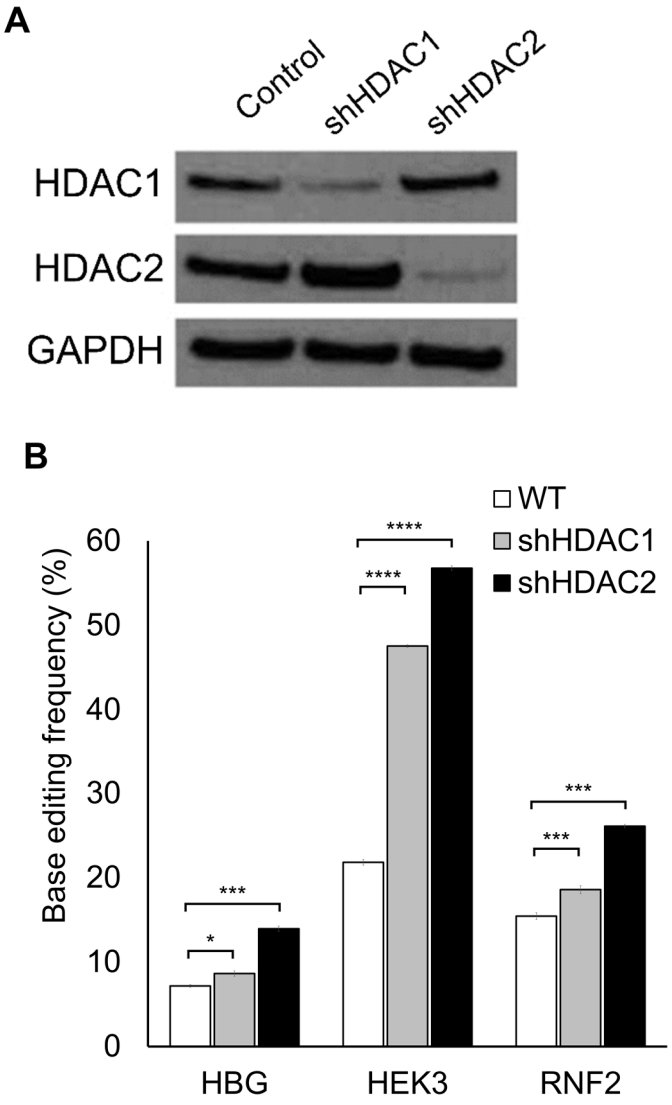

Figure 12. Inhibition of HDAC1 and HDAC2 expression by romidepsin improves adenine base editing efficiency

(A) Western blot analysis to confirm the expression levels of HDAC1 and HDAC2 in the HEK293T/17 cells expressing non-target (negative control), HDAC1, and HDAC2 targeting shRNAs. GAPDH was used as a loading control. (B) Base editing efficiency in HDAC1 and HDAC2 knockdown HEK293T/17 cells. Inhibition of HDAC1 and HDAC2 expression significantly increased adenine base editing

efficiency at all three endogenous target sites. Error bars indicate s.e.m (n = 3). Ns, not significant; $P \geq 0.05$; *$P < 0.05$; **$P < 0.01$; ***$P < 0.001$; ****$P < 0.0001$ (using two-tailed Student's t-test).

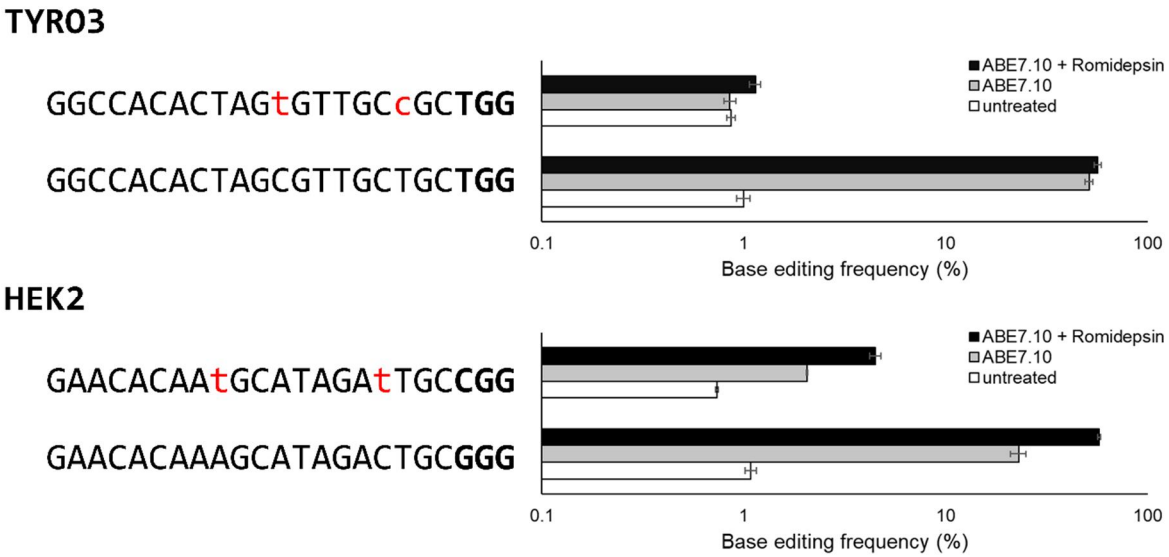

Figure 13. Analysis of off-target effect by romidepsin.

Base editing efficiencies were analyzed at off-target sites of gRNAs targeting TYRO3 and HEK2, which were previously well known, and two off-target sites contain 2 mismatches with their gRNAs (shown in red lowercase). Romidepsin increases adenine base editing efficiency in both on- and off-target sites. Error bars indicate SEM (n = 3).

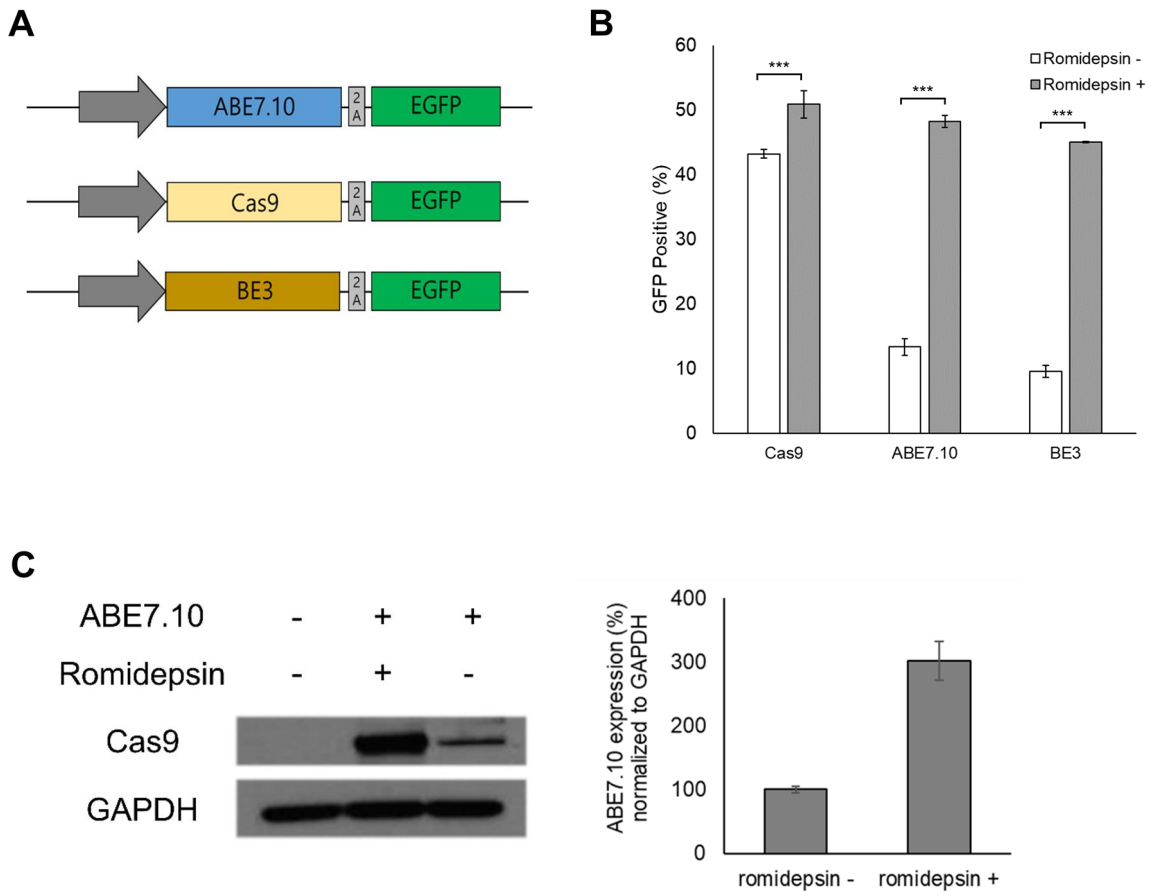

Figure 14. Romidepsin enhances adenine base editor protein expression level

(A) Schematic overview of ABE7.10-, Cas9-, BE3-2A-EGFP construct. The P2A-EGFP coding sequence was cloned behind the sequences of ABE7.10, Cas9, and BE3. (B) HEK293T/17 cells were transfected with Cas9/ABE7.10/BE3-2A-EGFP plasmid DNA and 10 nM of romidepsin treatment after 6h. After 72h of transfection, GFP-positive cells were analyzed using flow cytometry. (C) Western blot analysis to confirm ABE7.10 protein expression level by romidepsin treatment. ABE7.10 expression levels were increased in the presence of romidepsin. GAPDH is used as a loading control. Error bars indicate s.e.m (n = 3). ns, not significant;

P ≥ 0.05; *P < 0.05; **P < 0.01; ****P < 0.0001 (using two-tailed Student's t-test).

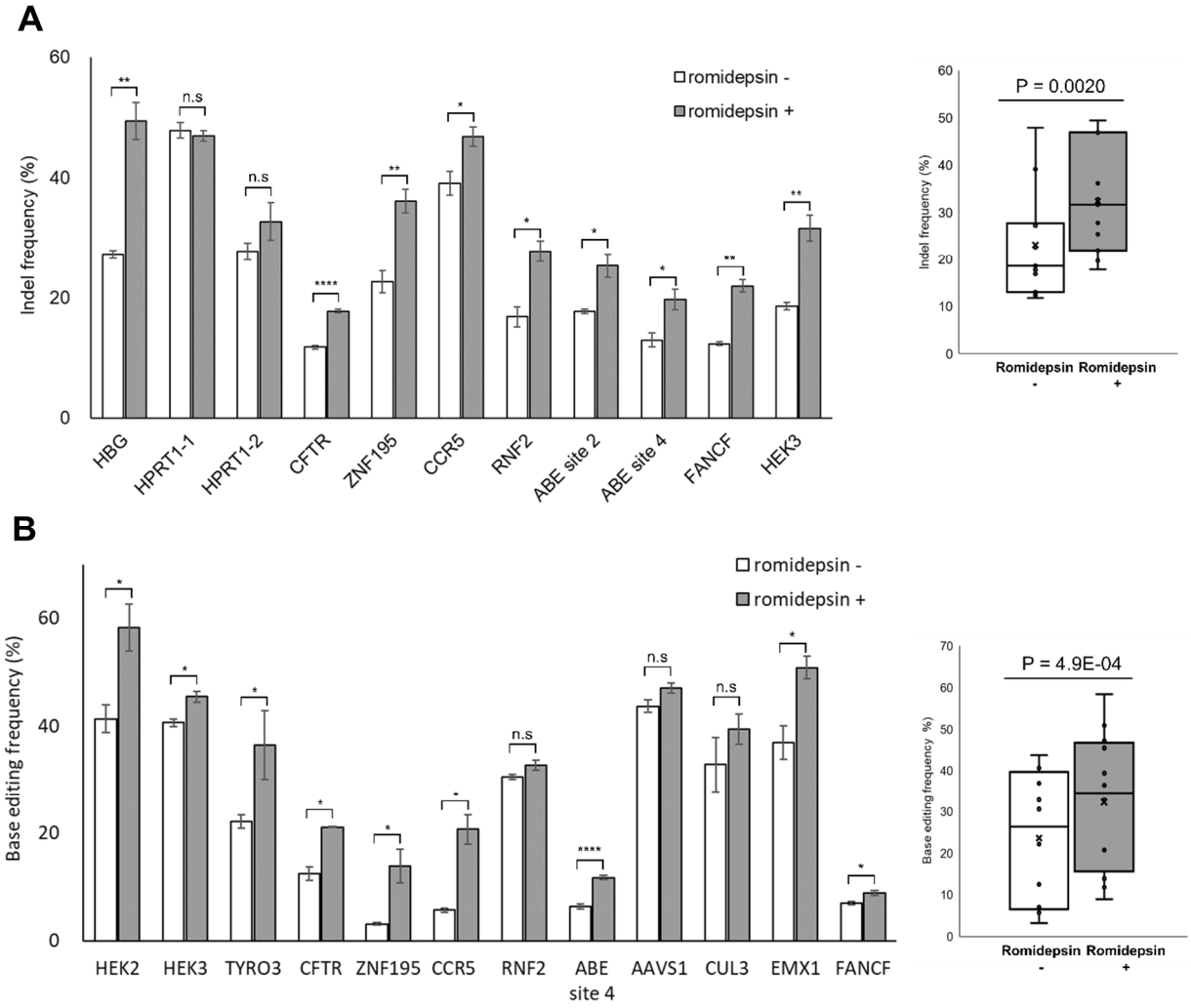

Figure 15. Assessment of Cas9- and BE3-mediated mutation frequencies by romidepsin treatment

To analyze Cas9- and BE3-mediated mutation frequency, HEK293T/17 cells were transfected with Cas9 or BE3 and gRNA plasmid DNA and treated 10 nM of romidepsin after 6h. 72h after transfection, (A) Cas9-mediated indel frequency and (B) BE3-mediated C to T conversion frequency was analyzed by targeted deep sequencing. The cumulative editing efficiency (right panel) is shown in a boxplot,

and the p−value was calculated using a two−tailed Wilcoxon signed rank test. Error bars indicate s.e.m. (n =2 or 3). ns, not significant; $P \geq 0.05$; *$P < 0.05$; **$P < 0.01$; ****$P < 0.0001$ (using two−tailed Student’ s t−test).

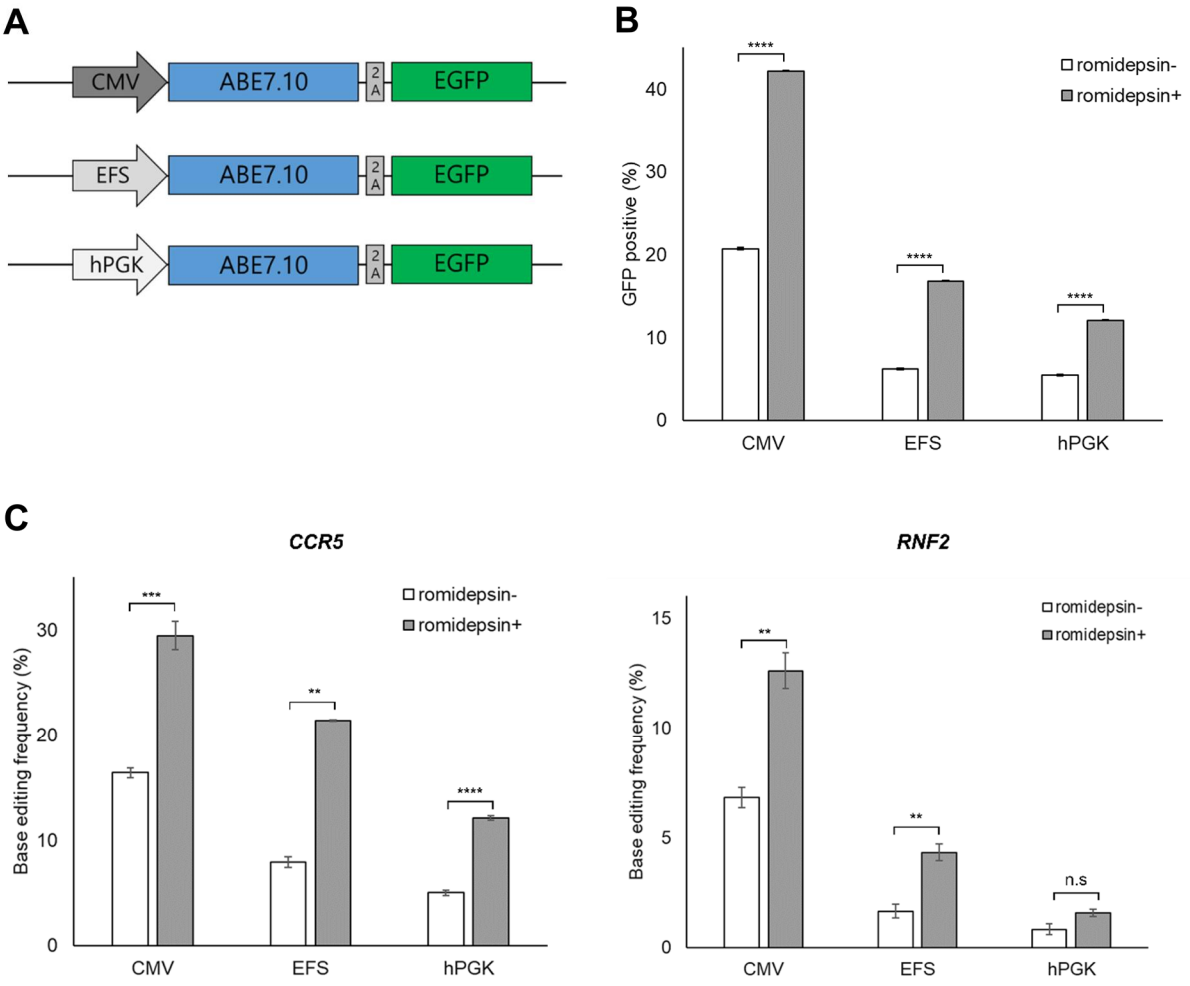

Figure 16. Romidepsin enhances alternative promote-driven ABE7.10 expression level.

(A) Scheme of CMV-, EFS-, hPGK-2A-ABE7.10 construct (B) HEK293T/17 cells were transfected with CMV/EFS/hPEG-ABE7.10-2A-EGFP plasmid DNA and 10 nM romidepsin treatment after 6h. After 72h of transfection, GFP-positive cells were analyzed using flow cytometry, and romidepsin increases protein expression levels of Cas-mediated editors. (B) CMV/EFS/hPEG-ABE7.10-2A-EGFP significantly increased base editing efficiency at three endogenous target

sites in the presence of romidepsin. Error bars indicate s.e.m (n = 3); ns, not significant; $P \geq 0.05$; *$P < 0.05$; **$P < 0.01$; ***$P < 0.001$; ****$P < 0.0001$ (using two-tailed Student's t-test).

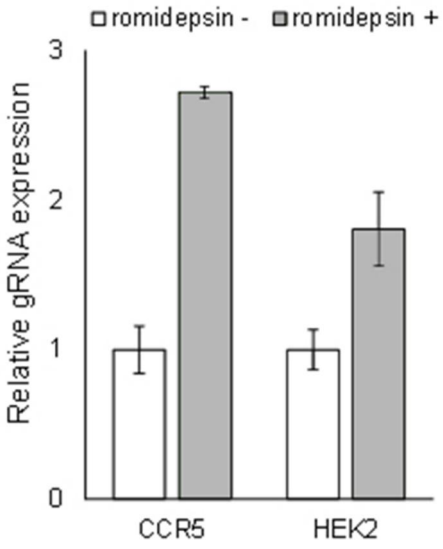

Figure 17. Romidepsin enhances a U6 promoter-driven gRNA expression level.

To analyze gRNA expression levels, total RNA was isolated from HEK293 cells transfected with 2 gRNA plasmid DNA, and quantitative real-time PCR was performed. Romidepsin improves U6 promoter-driven gRNA expression levels.

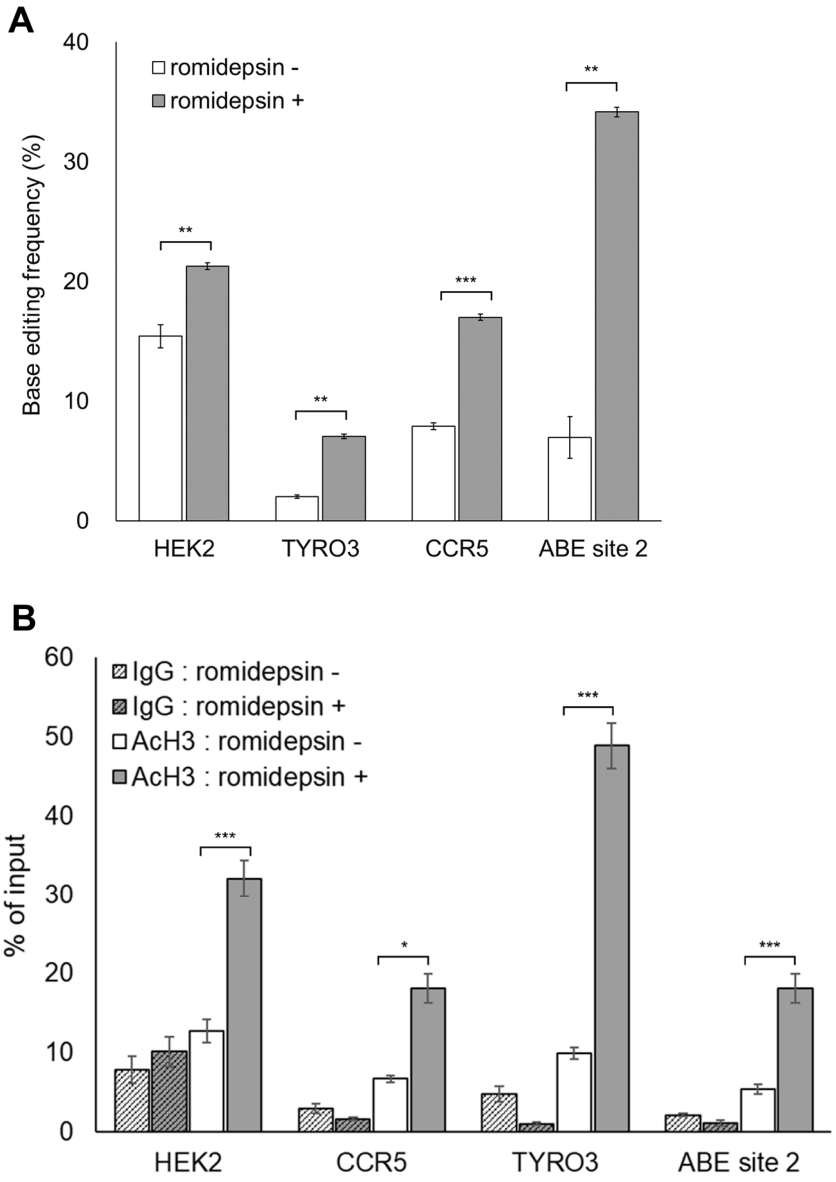

Figure 18. Romidepsin improves base editing efficiency by affecting the chromatin state.

(A) Romidepsin improves ABE7.10 RNP-mediated base editing efficiency at 4 endogenous target sites. (B) ChIP assay to evaluate histone acetylation. The acetylation percentages were increased at 4 endogenous target sites in the

presence of romidepsin. Error bars indicate s.e.m (n = 3); ns, not significant; $P \geq 0.05$; *$P < 0.05$; **$P < 0.01$; ***$P < 0.001$; ****$P < 0.0001$ (using two-tailed Student's t-test).

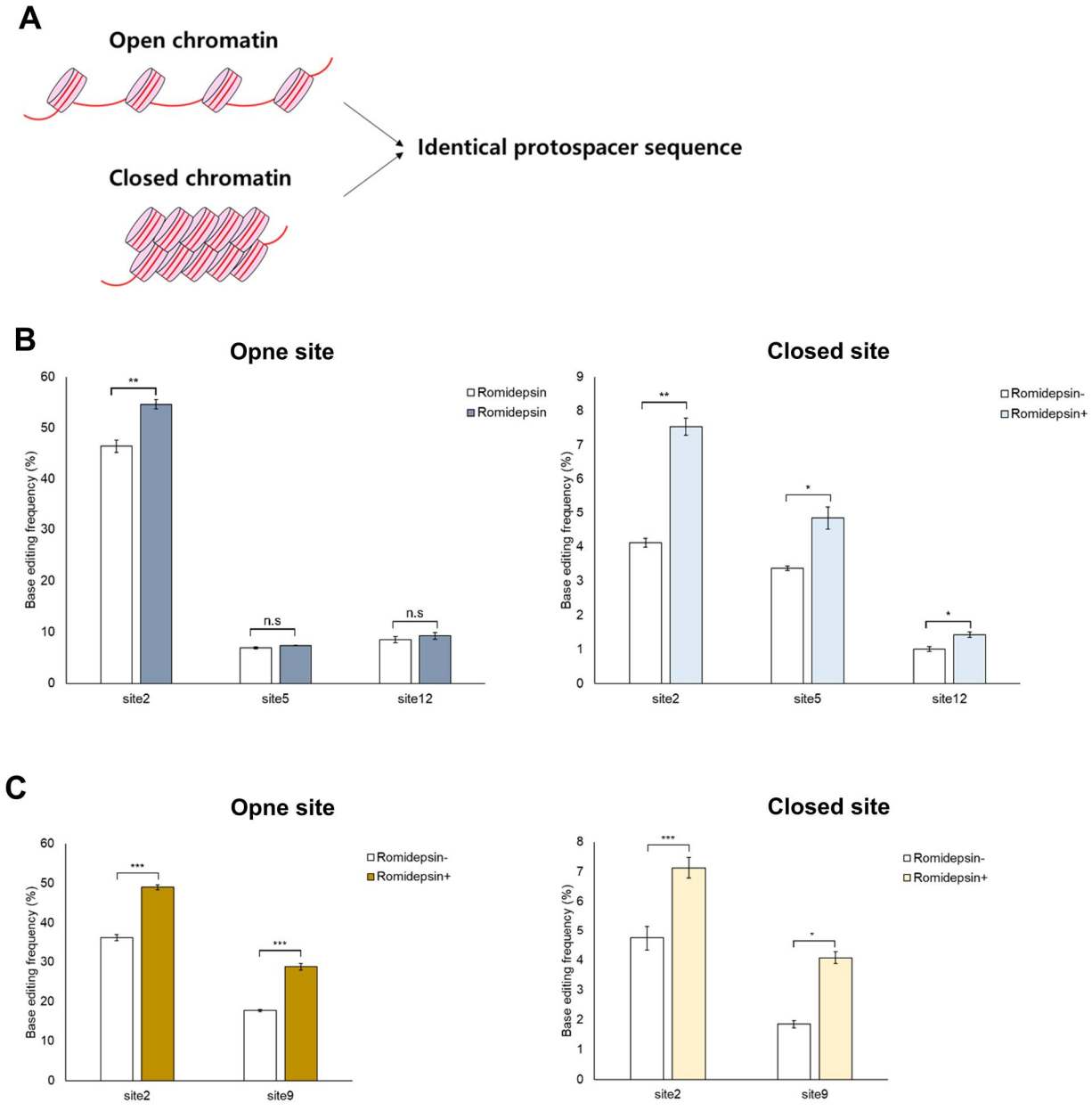

Figure 19. The effect of romidepsin in open and closed chromatin region.

(A) Scheme of evaluation of base editing efficiency in open and closed chromatin regions. The (B) ABE and (C) CBE-mediated base editing efficiencies by romidepsin treatment were evaluated in target sequences that are equally present in open and closed chromatin regions. HEK293T/17 cells were electroporated

quantified ABE or CBE protein and gRNA, and treated romidepsin after 6h. 72h after electroporation, base editing frequency was analyzed using targeted deep sequencing. Error bars indicate s.e.m (n = 3); ns, not significant; $P \geq 0.05$; $*P < 0.05$; $**P < 0.01$; $***P < 0.001$; $****P < 0.0001$ (using two-tailed Student's t-test).

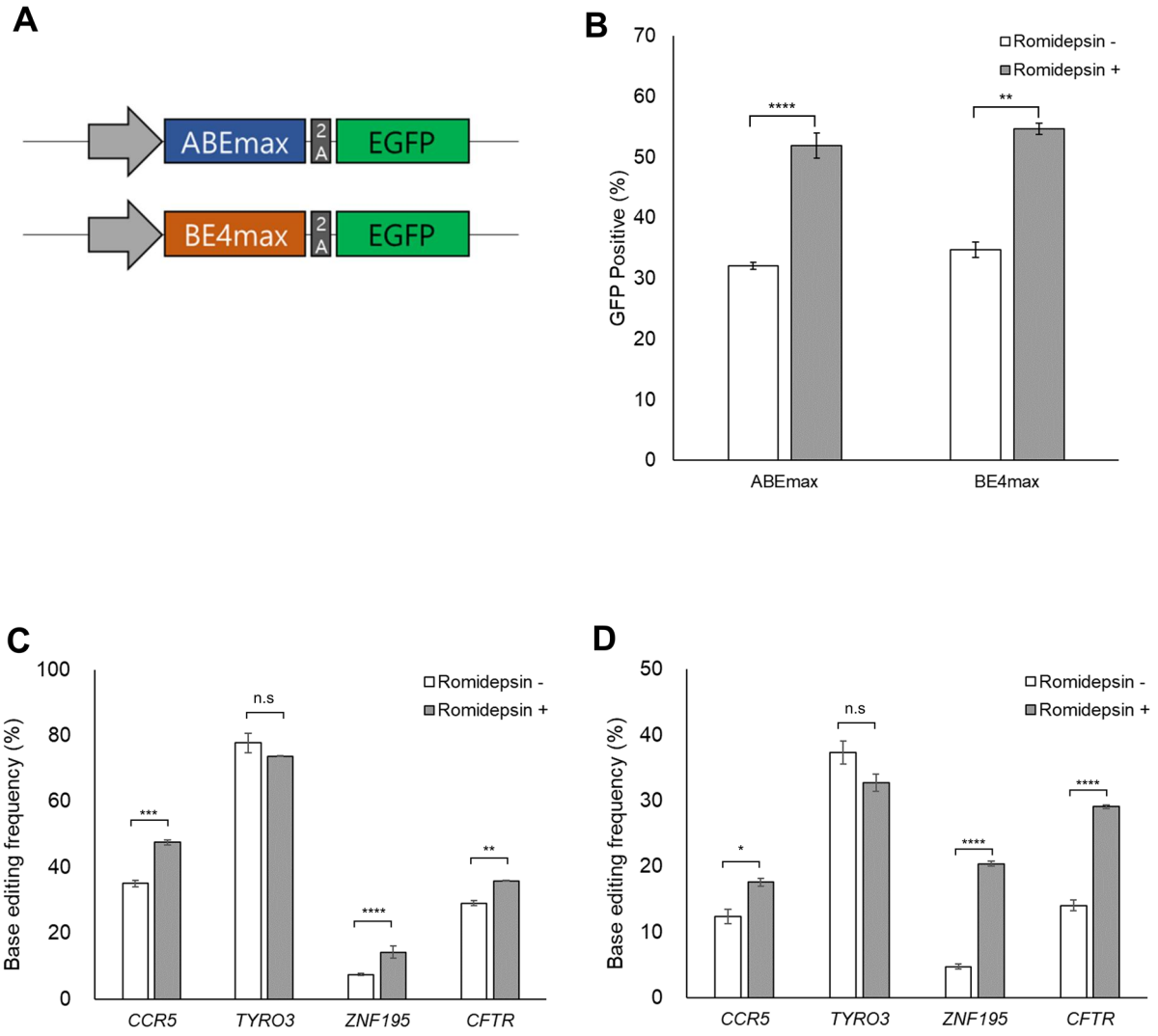

Figure 20. Romidepsin improves ABEmax- and BE4max-mediated base editing efficiency.

(A) HEK293T/17 cells were transfected with ABEmax/CBE4-2A-EGFP plasmid DNA and 10 nM romidepsin treatment after 6h. After 72h of transfection, GFP-positive cells were analyzed using flow cytometry, and romidepsin increases

protein expression levels of both ABEmax and CBE4max. Romidepsin increases the (B) ABEmax− and (C) CBE4ma−mediated base editing efficiency at 4 endogenous target sites. Error bars indicate s.e.m (n = 3), ns (not significant), $P \geq 0.05$; $*P < 0.05$; $**P < 0.01$; $***P < 0.001$; $****P < 0.0001$ (using two−tailed Student's t−test).

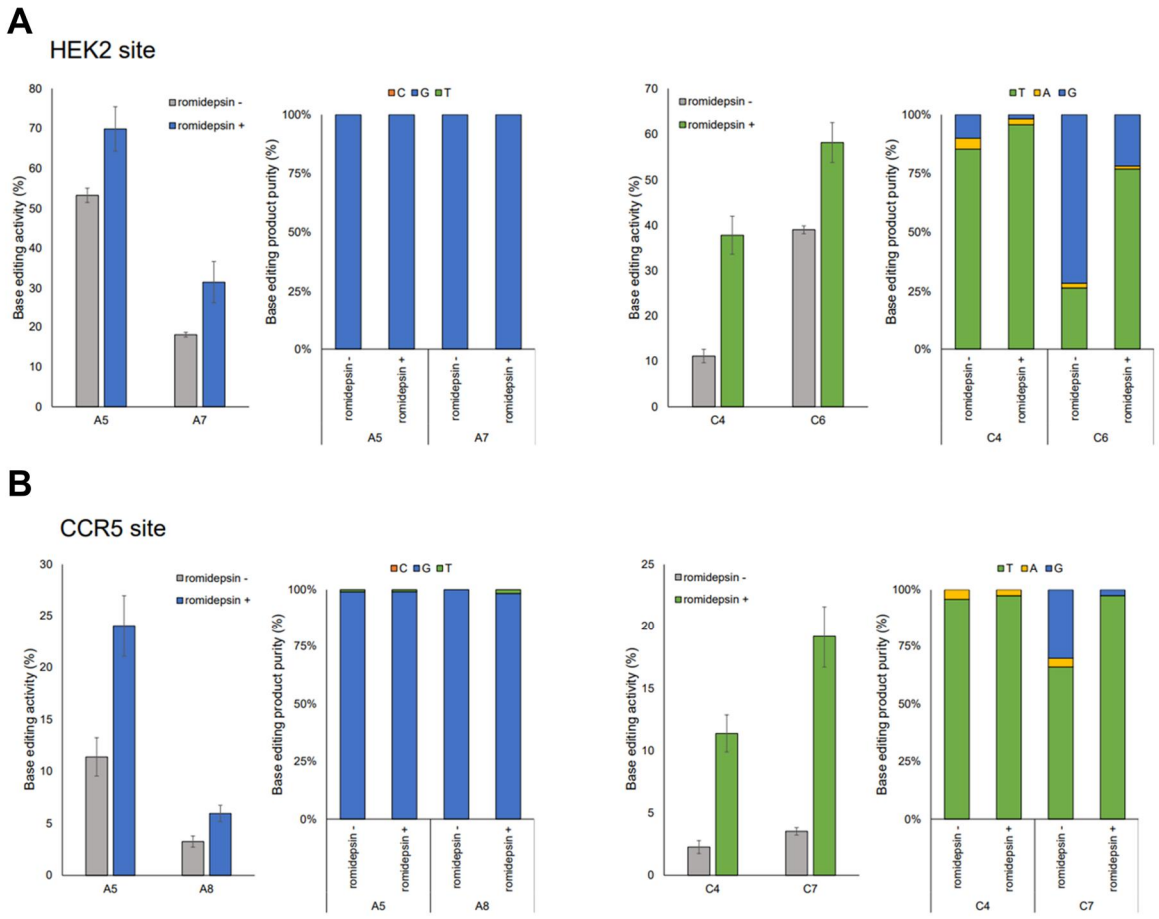

Figure 21. Effect of romidepsin on base editing product purity

Product purity was analyzed at (A) HEK2 and (B) CCR5 sites. The left panel is ABE, and the right panel is CBE editing results, and romidepsin improved the purity of CBE-mediated base editing products. Error bars indicate s.e.m. (n =3)

Table 1. List of target sequences of gRNA used in the study

Name	gRNA sequence (5' to 3' w/o PAM)
GFP reporter	GCTCTACACCATGGTGGCGA
CCR5	TGACATCAATTATTATACAT
HEK2	GAACACAAAGCATAGACTGC
HEK3	GGCCCAGACTGAGCACGTGA
TYRO3	GGCCACACTAGCGTTGCTGC
HBG	GTGGGGAAGGGGCCCCCAAG
HPRT1-1	GAAAGGGTGTTTATTCCTCA
HRPT1-2	GATGTGATGAAGGAGATGGG
ZNF195	CAGAAACATTGAGGCCTGGC
CFTR	TGAGATCTTTGACAGTCATT
ABE site 2	GAGTATGAGGCATAGACTGC
ABE site 4	GAGCAAAGAGAATAGACTGT
RNF2	GTCATCTTAGTCATTACCTG
AAVS1	GCTGACTCAGAGACCCTGAG
CUL3	GTAAACCTGGAATAACACGA
EMX1	GTCACCTCCAATGACTAGGG
FANCF	GGAATCCCTTCTGCAGCACC
TYRO3 Off-target	GGCCACACTAGTGTTGCCGC
HEK2 off-target	GAACACAATGCATAGATTGC
site_2(Dig-seq)	TCACAGATGCCAAGCAGCTG
site_5(Dig-seq)	CCTGGGAGGCCAGGGTCACA
site_9(Dig-seq)	GAGCCTTGCAGCTTCAGCCT
site_12(Dig-seq)	TGAATTGAGGCAGTAGCCTC

Table 2. List of primer sequences used in the study

Targeted deep seequencing			
Name	**PCR**	**Forward**	**Reverse**
GFP reporter	1st	TATAAGCAGAGCTGGTTTAG	GGACACGCTGAACTTGTGGC
	2nd	ACACTCTTTCCCTACACGACGCTCTTCCGATCTTGA ACCGTCAGATCCGCTAG	GTGACTGGAGTTCAGACGTGTGCTCTTCCGATC TCCGTTTACGTCGCCGTCCAG
HEK2	1st	GAGGCCCATTAACGTTTGGC	AGACTCAAAACCTGGCCCAC
	2nd	ACACTCTTTCCCTACACGACGCTCTTCCGATCTAGA CCTGGCTGAGCTAACTG	GTGACTGGAGTTCAGACGTGTGCTCTTCCGATC TTCCAGCCCCATCTGTCAAAC
HEK3	1st	CGCCCATGCAATTAGTCTAT	GCCAAACTTGTCAACCAGTA
	2nd	ACACTCTTTCCCTACACGACGCTCTTCCGATCTCAT TTGTAGGCTTGATGCTT	GTGACTGGAGTTCAGACGTGTGCTCTTCCGATC TCACATACTAGCCCCTGTCTA
CCR5	1st	CTCCATGGTGCTATAGAGCA	GCCCTGTCAAGAGTTGACAC
	2nd	ACACTCTTTCCCTACACGACGCTCTTCCGATCTGAG GGCAACTAAATACATTCTAGGAC	GTGACTGGAGTTCAGACGTGTGCTCTTCCGATC TCCAAAGATGAACACCAGTGA
TYRO3	1st	GAGGCAACCTCTCTCCACAG	CCAGAGCACCCCATGATAAG
	2nd	ACACTCTTTCCCTACACGACGCTCTTCCGATCTTCC CTACTGGGCACTGATTC	GTGACTGGAGTTCAGACGTGTGCTCTTCCGATC TTCCCTGTCAACAAAGTGCTG
CFTR	1st	TTGACATGCCAACAGAAGGT	TCTGCTAACACATTGCTTCAGG
	2nd	ACACTCTTTCCCTACACGACGCTCTTCCGATCTCGA TCTGTGAGCCGAGTCTT	GTGACTGGAGTTCAGACGTGTGCTCTTCCGATC TTCTGGCCAGGACTTATTGAGA
HBG	1st	GATGGGAGAAGGAAACTAGC	GCCTCACTGGATACTCTAAG
	2nd	ACACTCTTTCCCTACACGACGCTCTTCCGATCTTAG AGAAAAACTGGAATGAC	GTGACTGGAGTTCAGACGTGTGCTCTTCCGATC TCTCTAAGACTATTGGTCAAG
HPRT_1-1	1st	GTATCCTGTAATGCTCTCAT	CCTAGTTTATGTTCAAATAGC
	2nd	ACACTCTTTCCCTACACGACGCTCTTCCGATCTCAG ATTAGTGATGATGAACC	GTGACTGGAGTTCAGACGTGTGCTCTTCCGATC TATAGCAAGTACTCAGAACAG
HPRT_1-2	1st	TCACTATATTGCCCAGGTTG	ATCTACAGTCATAGGAATGGATC
	2nd	ACACTCTTTCCCTACACGACGCTCTTCCGATCTGGT GTGGAAGTTTAATGACT	GTGACTGGAGTTCAGACGTGTGCTCTTCCGATC TAGTGCTTTGATGTAATCCAG
ZNF195	1st	AAACAGACTGAGAAACTGAGGT	CTCCACTTCCCAGGTTCAGG
	2nd	ACACTCTTTCCCTACACGACGCTCTTCCGATCTGCA GCAAGTGAAAAGCAAGG	GTGACTGGAGTTCAGACGTGTGCTCTTCCGATC TGGGACTACAAGTGTGCAACA
ABE site2	1st	AGGTGGCAAGGGAACAAAGT	TGCAATCCCAGCTACTTGGG
	2nd	ACACTCTTTCCCTACACGACGCTCTTCCGATCTCCC TGAGATACAGTCACGAGG	GTGACTGGAGTTCAGACGTGTGCTCTTCCGATC TCCTGAAATGCTGTGCGTGTC
ABE site4	1st	ATCTTGGCTCACTGCAAGCT	GTAGGAGAGGGAGCTGTCCA
	2nd	ACACTCTTTCCCTACACGACGCTCTTCCGATCTAGC CAGGATGGTCTCGATCT	GTGACTGGAGTTCAGACGTGTGCTCTTCCGATC TACAGAGAGTTACTGCTCAGACA
RNF2	1st	CTCTCTTCTTTATTTCCAGC	GTGTTAGCCAACATACAGAA
	2nd	ACACTCTTTCCCTACACGACGCTCTTCCGATCTACA AACGGAACTCAACCATT	GTGACTGGAGTTCAGACGTGTGCTCTTCCGATC TTACAGAAGTCAGGAATGCTT
AAVS1	1st	CCCAACTCACCTCATCACCT	GCTCACTGCAACCTCCAACT
	2nd	ACACTCTTTCCCTACACGACGCTCTTCCGATCTGGC CCAGACTAGCCCAGTTGT	GTGACTGGAGTTCAGACGTGTGCTCTTCCGATC TCCACCTGCCTTGGCCTCTCA
CUL3	1st	CCATCCTTTGCTGGCATTAT	AGTAGGGATGGGGTTTCACC
	2nd	ACACTCTTTCCCTACACGACGCTCTTCCGATCTTTG GGAGCACTTCCAGGTTCACT	GTGACTGGAGTTCAGACGTGTGCTCTTCCGATC TCTGCACTCCAGCCTTGGTGACAG
EMX1	1st	GAGGAGCTAGGATGCACAGC	AATCTACCACCCCAGGCTCT
	2nd	ACACTCTTTCCCTACACGACGCTCTTCCGATCTGAA GCAGGCCAATGGGGAGG	GTGACTGGAGTTCAGACGTGTGCTCTTCCGATC TCTTGTCCCTCTGTCAATGGCGG

FANCF	1st	TCCAGAGCCGTGCGAAT	CGGATAAAGACGCTGGGA
	2nd	ACACTCTTTCCCTACACGACGCTCTTCCGATCTAGG TGCTGACGTAGGTAGT	GTGACTGGAGTTCAGACGTGTGCTCTTCCGATC TCCAATCAGTACGCAGAGAG
TYRO3 Off-target	1st	TCCCGGAGCAGGCAGGTAAA	AATGCCTGGCCTCTTCTCGC
	2nd	ACACTCTTTCCCTACACGACGCTCTTCCGATCTACC ACAACAGCCAGGACTTC	GTGACTGGAGTTCAGACGTGTGCTCTTCCGATC TTCTCGCATAGCCACTGTTCT
HEK2 Off-target	1st	GAGATTCAATCTGACAGATC	TTGTGAAACAGAAATGTCAG
	2nd	ACACTCTTTCCCTACACGACGCTCTTCCGATCTATC TGTAACTAGAACAATGG	GTGACTGGAGTTCAGACGTGTGCTCTTCCGATC TCAGTTATTATGAGAATCATT
site_2(Dig-seq)	1st	TGGAGGTCGGTACTTAGTTT	TCGCTATGTCAAAGATCCTT
	2nd	ACACTCTTTCCCTACACGACGCTCTTCCGATCTGGG ATGAAAATAGGGAGGAA	GTGACTGGAGTTCAGACGTGTGCTCTTCCGATC TTCTGATAAACGGCAGTATGG
site_5(Dig-seq)	1st	AACTGATGGTGAGGCTAG	CTCTACAAGGAAACTCTTCA
	2nd	ACACTCTTTCCCTACACGACGCTCTTCCGATCTTGC ATGGTAGGTCACTCA	GTGACTGGAGTTCAGACGTGTGCTCTTCCGATC TTCCTCAAGCCAGCAAA
site_9(Dig-seq)	1st	CTCTCCATGAGGTTGA	AAGAGGTGGAGGCTAA
	2nd	ACACTCTTTCCCTACACGACGCTCTTCCGATCTTGC TGGGTTCTGAGAGTAAG	GTGACTGGAGTTCAGACGTGTGCTCTTCCGATC TTCACCTTCTCTTGGATCTGG
site_12(Dig-seq)	1st	GATAAGGGAGGGGTTCTT	TGTTGAGACAAGTGTGAACC
	2nd	ACACTCTTTCCCTACACGACGCTCTTCCGATCTTGA CTCACTCCCTCTGCT	GTGACTGGAGTTCAGACGTGTGCTCTTCCGATC TAAGTGTGAACCTGCCAGT

Chip-qPCR

Name	PCR	Forward	Reverse
HEK2	1st	TTGGCCCTTCAAGTTACTGC	AAGGGGGAAAAATTGTCCAG
Site 2	1st	TGCGTGGAGTTCATGGAGTA	GAGGAGGAGTTCGCAGTGAG
TYRO3	1st	ACTGTGATCCTGGGAGTGCT	CGGAGAGCCTACCTGAACTG
CCR5	1st	TTATGCACAGGGTGGAACAA	AGCATAGTGAGCCCAGAAGG

quantitative Real time PCR

Name	PCR	Forward	Reverse
CCR5 gRNA	1st	ACATGTTTTAGAGCTAGAAATAGCAA	CGGTGCCACTTTTTCAAGTT
EHK2 gRNA	1st	CACAAAGCATAGACTGCGTTTTA	

Table 3. Top 30 drugs in small molecule drug screening

100 nM Treatment			500 nM Treatment		
Rank	**Drugs**	**FC**	**Rank**	**Drugs**	**FC**
1	**Romidepsin (FK228, Depsipeptide)**	**5.33**	1	**Romidepsin (FK228, Depsipeptide)**	**7.79**
2	Bexarotene	3.87	2	PHA-665752	5.33
3	PHA-665752	3.19	3	PD173955	5.00
4	Lapatinib	3.15	4	CPI-203	4.90
5	Cyclophosphamide monohydrate	3.07	5	Obatoclax mesylate (GX15-070)	4.81
6	**Quisinostat**	**3.01**	6	MLN2238	4.06
7	Crenolanib (CP-868596)	3.00	7	MLN9708	3.98
8	MLN9708	2.75	8	Idarubicin HCl	3.95
9	Vinorelbine Tartrate	2.75	9	Mitoxantrone	3.55
10	MLN2238	2.59	10	Mitoxantrone HCl	3.52
11	Sunitinib Malate (Sutent)	2.46	11	Vinorelbine Tartrate	3.29
12	Daunorubicin HCl (Daunomycin HCl)	2.30	12	**Quisinostat**	**3.09**
13	Gemcitabine (Gemzar)	2.27	13	Nocodazole	3.02
14	PD173955	2.26	14	Saracatinib (AZD0530)	2.72
15	Mitoxantrone	2.21	15	Bosutinib (SKI-606)	2.68
16	Idarubicin HCl	2.15	16	KX2-391	2.59
17	Entinostat (MS-275, SNDX-275)	2.15	17	Geldanamycin	2.58
18	Azathioprine (Azasan, Imuran)	2.14	18	LY2874455	2.58
19	Bosutinib (SKI-606)	2.12	19	Teniposide (Vumon)	2.47
20	**Trichostatin A (TSA)**	**2.07**	20	PF-3758309	2.47
21	Nocodazole	2.02	21	HSP990 (NVP-HSP990)	2.47
22	Mitoxantrone HCl	2.02	22	Sunitinib Malate (Sutent)	2.46
23	Bortezomib (Velcade)	2.02	23	**Abexinostat**	**2.44**
24	**Abexinostat**	**2.00**	24	Anagrelide HCl	2.39
25	Dasatinib (BMS-354825)	1.99	25	BX-795	2.30
26	Mesna (Uromitexan, Mesnex)	1.99	26	Ro3280	2.22
27	Brivanib (BMS-540215)	1.97	27	Crenolanib (CP-868596)	2.22
28	CPI-203	1.96	28	GSK923295	2.21
29	KU-55933	1.94	29	**Trichostatin A (TSA)**	**2.19**
30	BMS-599626 (AC480)	1.92	30	BI-847325	2.16

Table 4. List of off−target sites

Target site		Genoem position	Target sequence	PAM	Mismatch
TYRO3	on-target	chr15:41565067	GGCCACACTAGCGTTGCTGC	TGG	0
	off-target	chr15:76260974	GGCCACACTAGtGTTGCcGC	TGG	2
HEK2	on-target	chr5:87944779	GAACACAAAGCATAGACTGC	GGG	0
	off-target	chr4:89601015	GAACACAAtGCATAGAtTGC	CGG	2

4. DISCUSSION

In this study, a fluorescent reporter system was developed that detects fluorescent signals through doxycycline-inducible adenine base editing. Using the reporter system, small-molecule screening was performed, and candidates that improve adenine base editing efficiency were identified. In a small molecule screen, HDAC inhibitors, including romidepsin, were found to increase the fluorescence signal. As a result, romidepsin significantly improved adenine base editing efficiency at endogenous target sites. These effects have been demonstrated that romidepsin increases ABE7.10 protein and gRNA expression and converts to an open chromatin state (euchromatin) at the target site. In addition, ABEmax and BE4max, which were engineered to enhance base editing efficiency, also showed improved base editing efficiency.

Previous studies have reported that poor expression of ABE7.10 and BE3 is a bottleneck for the base editing efficiency and optimization of codon usage and NLS sequence was developed BE variants with improved efficiency, namely ABEmax and BE4max [40]. Here, romidepsin increased ABE7.10 and BE3 protein expression levels, which improved base editing efficiency at endogenous target sites. These results are consistent with previous findings that enhancing ABE7.10 and BE3 expression improves base editing efficiency. Romidepsin also showed enhanced ABEmax and BE4max expression levels and increased base editing efficiency, but not at sites with high BE activity. As shown in Figure. 8A and 20 C,

D results, at the TYRO3 site, romidepsin increased ABE7.10 and BE3-mediated base editing efficiency and induced chromatin state conversions but did not increase ABEmax and BE4max-mediated base editing efficiency. This suggests that the mechanism of romidepsin for improving base editing efficiency may be complicated and that the effects may differ depending on the target site or delivery material.

Eukaryotic genomic DNA is compressed by stacking on histone proteins, forming a compact structure, in contrast to prokaryotic DNA. Previous studies have reported that nucleosome and chromatin affect Cas9 activity by limiting the accessibility of its target site [68, 72], but whether it affects BE activity is unknown. Romidepsin, identified through drug screening, is an HDAC1 and HDAC2 inhibitor. Recently, Liu et al. reported that inhibitor of HDAC1 and HDAC2 expression enhances Cas9-mediated genome editing [73]. This demonstrated that the conversion of heterochromatin (closed chromatin) to euchromatin (open chromatin) promotes Cas9 protein accessibility and binding, improving genome editing efficiency. These results are consistent with the findings that romidepsin increases Cas9-mediated genome editing efficiency, as shown in Figure. 15A. It is not yet known if the chromatin state affects base editing activity. ABE7.10 RNPs were delivered into HEK293T/17 cells to evaluate whether chromatin state converting by romidepsin affects the ABE activity. Delivering RNPs, a quantified protein and gRNA complex, can evaluate the base editing efficiency according to the chromatin state. In RNP delivery, romidepsin has been shown to enhance base editing efficiency and induce an open state of chromatin, indicating that the chromatin state may affect base editor activity. In addition, RNPs delivery, which has the benefits

of rapid operation and degradation, high efficiency, low off-target effect, and toxicity, provides the usefulness of HDCA inhibitors in RNP-mediated therapeutic trials. However, for further investigation in chromatin regions, the effects of romidepsin were identified on the identical target sequence in both open and closed chromatin regions. ABE improved base editing efficiency by romidepsin treatment in the closed chromatin region, whereas CBE improved base editing efficiency in both open and closed chromatin regions. These results indicate that the chromatin state can improve the efficiency of base editing due to improved Cas RNP accessibility, but it may also be a phenomenon caused by other factors that have not yet been identified. Therefore, it is necessary to investigate the mechanism of the base editor in the chromatin region through further studies.

On the other hand, romidepsin treatment has increased the base editing frequency at both on- and off-target sites. These effects reflect the ability of HDAC inhibitors to enhance ABE protein expression and convert the chromatin structure of the genome to an open state overall. Further studies should investigate the effect of the HDAC inhibitor on the off-target effects. Especially, the off-target effect is the most significant issue in treatment trials, and this issue can be overcome by using BE variants engineered to reduce the off-target effect together with HDAC inhibitor treatment.

BEs can produce byproducts from base editing results. ABE induces high-purity A to G conversion, but CBE produces byproducts such as C to non-T, resulting in unwanted editing. To evaluate the improvement of the purity of the base editor by

romidepsin, base editing purity was analyzed, and the purity of CBE was improved. Previous studies have reported that HDAC inhibitors induce UNG2 depletion [74]. Therefore, these results suggest that the UGI of CBE and HDAC inhibitor may have improved purity due to the strong inhibition of UNG.

This study is the first case of a small molecule strategy to improve base editor efficiency and has provided insights for subsequent studies. Tianyuan Z. et al. identified a small molecule drug that enhances base editing efficiency using a reporter system, which was an HDAC inhibitor [75]. In addition, the purity of CBE was significantly improved by HDAC inhibitors. These results are consistent with the findings of this study that HDAC inhibitors can improve base editing efficiency and purity. In addition, more recently, a new genome manipulation tool, the prime editor (PE), has been developed. PE consists of an effector form in which reverse transcriptase is fused to nCas9 and an extended pegRNA containing the sequence to be edited. PE nicks the target DNA by nCas9 and exposes a DNA flap with 3−OH groups priming the RT template of pegRNA. This forms an intermediate containing a 3' flap with the edited sequence and a 5' flap with the unedited sequence, and the 5' flap is cleaved by the 5' exonuclease. This eventually induces hybridization of the 3' flap and allows for desired modifications by DNA ligation and repair. This PE system enables effective gene editing by designing pegRNAs to include the desired editing sequence in the RT template, enabling insertions, deletions, and all 12−point mutations. Recently, Nan Liu et al. reported that HDAC inhibitors also influence improving the efficiency of the PE system [76]. Therefore, these results support the

findings of this study that the effect of HDAC inhibitors affects the efficiency of CRISPR-mediated genome editing.

To summarize the above, HDAC inhibitors show improved base editing efficiency at endogenous target sites. These improvements are explained by affecting protein expression and chromatin state, which contribute to enhanced base editing activity. It can also support the use of romidepsin as a strategy to increase base editing efficiency in vivo in therapeutic applications.

5. REFERENCES

1. Barrangou, R., et al., *CRISPR provides acquired resistance against viruses in prokaryotes.* Science, 2007. **315**(5819): p. 1709-12.

2. Marraffini, L.A., *CRISPR-Cas immunity in prokaryotes.* Nature, 2015. **526**(7571): p. 55-61.

3. Gasiunas, G., et al., *Cas9-crRNA ribonucleoprotein complex mediates specific DNA cleavage for adaptive immunity in bacteria.* Proc Natl Acad Sci U S A, 2012. **109**(39): p. E2579-86.

4. Andersson, A.F. and J.F. Banfield, *Virus population dynamics and acquired virus resistance in natural microbial communities.* Science, 2008. **320**(5879): p. 1047-50.

5. Makarova, K.S., et al., *A putative RNA-interference-based immune system in prokaryotes: computational analysis of the predicted enzymatic machinery, functional analogies with eukaryotic RNAi, and hypothetical mechanisms of action.* Biol Direct, 2006. **1**: p. 7.

6. Jinek, M., et al., *A programmable dual-RNA-guided DNA endonuclease in adaptive bacterial immunity.* Science, 2012. **337**(6096): p. 816-21.

7. Sternberg, S.H., et al., *DNA interrogation by the CRISPR RNA-guided endonuclease Cas9.* Nature, 2014. **507**(7490): p. 62-7.

8. Ran, F.A., et al., *In vivo genome editing using Staphylococcus aureus Cas9.* Nature, 2015. **520**(7546): p. 186-91.

9. Hou, Z., et al., *Efficient genome engineering in human pluripotent stem cells using Cas9 from Neisseria meningitidis.* Proc Natl Acad Sci U S A, 2013. **110**(39): p. 15644-9.

10. Fonfara, I., et al., *Phylogeny of Cas9 determines functional exchangeability of dual-RNA and Cas9 among orthologous type II CRISPR-Cas systems.* Nucleic Acids Res, 2014. **42**(4): p. 2577-90.

11. Hu, J.H., et al., *Evolved Cas9 variants with broad PAM compatibility and high DNA specificity.* Nature, 2018. **556**(7699): p. 57-63.

12. Kleinstiver, B.P., et al., *Engineered CRISPR-Cas9 nucleases with altered PAM specificities.* Nature, 2015. **523**(7561): p. 481-5.

13. Walton, R.T., et al., *Unconstrained genome targeting with near-PAMless engineered CRISPR-Cas9 variants.* Science, 2020. **368**(6488): p. 290-296.

14. Cong, L., et al., *Multiplex genome engineering using CRISPR/Cas systems.* Science, 2013. **339**(6121): p. 819-23.

15. Jinek, M., et al., *RNA-programmed genome editing in human cells.* Elife, 2013. **2**: p. e00471.

16. Mali, P., et al., *RNA-guided human genome engineering via Cas9.* Science, 2013. **339**(6121): p. 823-6.

17. Jiang, F. and J.A. Doudna, *CRISPR-Cas9 Structures and Mechanisms.* Annu Rev Biophys, 2017. **46**: p. 505-529.

18. Ran, F.A., et al., *Genome engineering using the CRISPR-Cas9 system.* Nat Protoc, 2013. **8**(11): p. 2281-2308.

19. Nishimasu, H., et al., *Crystal structure of Cas9 in complex with guide RNA and target DNA.* Cell, 2014. **156**(5): p. 935-49.

20. Cho, S.W., et al., *Analysis of off-target effects of CRISPR/Cas-derived RNA-guided endonucleases and nickases.* Genome Res, 2014. **24**(1): p. 132-41.

21. Shen, B., et al., *Efficient genome modification by CRISPR-Cas9 nickase with minimal off-target effects.* Nat Methods, 2014. **11**(4): p. 399-402.

22. Chen, B., et al., *Dynamic imaging of genomic loci in living human cells by an optimized CRISPR/Cas system.* Cell, 2013. **155**(7): p. 1479-91.

23. Larson, M.H., et al., *CRISPR interference (CRISPRi) for sequence-specific control of gene expression.* Nat Protoc, 2013. **8**(11): p. 2180-96.

24. Lau, C.H. and Y. Suh, *In vivo epigenome editing and transcriptional modulation using CRISPR technology.* Transgenic Res, 2018. **27**(6): p. 489-509.

25. Ma, H., et al., *Multicolor CRISPR labeling of chromosomal loci in human cells.* Proc Natl Acad Sci U S A, 2015. **112**(10): p. 3002-7.

26. Li, M., et al., *Reassessment of the Four Yield-related Genes Gn1a, DEP1, GS3, and IPA1 in Rice Using a CRISPR/Cas9 System.* Front Plant Sci, 2016. **7**: p. 377.

27. Zsögön, A., et al., *De novo domestication of wild tomato using genome editing.* Nat Biotechnol, 2018.

28. Hsu, P.D., E.S. Lander, and F. Zhang, *Development and applications of CRISPR-Cas9 for genome engineering.* Cell, 2014. **157**(6): p. 1262-1278.

29. Ma, C.C., et al., *The approved gene therapy drugs worldwide: from 1998 to 2019.* Biotechnol Adv, 2020. **40**: p. 107502.

30. Li, H.L., et al., *Precise correction of the dystrophin gene in duchenne muscular dystrophy patient induced pluripotent stem cells by TALEN and CRISPR-Cas9.* Stem Cell Reports, 2015. **4**(1): p. 143-154.

31. Loayza-Puch, F., et al., *Tumour-specific proline vulnerability uncovered by differential ribosome codon reading.* Nature, 2016. **530**(7591): p. 490-4.

32. Joo, M.S., et al., *AMPK Facilitates Nuclear Accumulation of Nrf2 by Phosphorylating at Serine 550.* Mol Cell Biol, 2016. **36**(14): p. 1931-42.

33. Haapaniemi, E., et al., *CRISPR-Cas9 genome editing induces a p53-mediated DNA damage response.* Nat Med, 2018. **24**(7): p. 927-930.

34. Ihry, R.J., et al., *p53 inhibits CRISPR-Cas9 engineering in human pluripotent stem cells.* Nat Med, 2018. **24**(7): p. 939-946.

35. Stadtmauer, E.A., et al., *CRISPR-engineered T cells in patients with refractory cancer.* Science, 2020. **367**(6481).

36. Rees, H.A. and D.R. Liu, *Base editing: precision chemistry on the genome and transcriptome of living cells.* Nat Rev Genet, 2018. **19**(12): p. 770-788.

37. Komor, A.C., et al., *Programmable editing of a target base in genomic DNA without double-stranded DNA cleavage.* Nature, 2016. **533**(7603): p. 420-4.

38. Komor, A.C., et al., *Improved base excision repair inhibition and bacteriophage Mu Gam protein yields C:G-to-T:A base editors with higher efficiency and product purity.* Sci Adv, 2017. **3**(8): p. eaao4774.

39. Gaudelli, N.M., et al., *Programmable base editing of A•T to G•C in genomic DNA without DNA cleavage.* Nature, 2017. **551**(7681): p. 464-471.

40. Koblan, L.W., et al., *Improving cytidine and adenine base editors by expression optimization and ancestral reconstruction.* Nat Biotechnol, 2018. **36**(9): p. 843-846.

41. Jiang, W., et al., *Demonstration of CRISPR/Cas9/sgRNA-mediated targeted gene modification in Arabidopsis, tobacco, sorghum and rice.* Nucleic Acids Res, 2013. **41**(20): p. e188.

42. Kim, J.M., et al., *Genotyping with CRISPR-Cas-derived RNA-guided endonucleases.* Nat Commun, 2014. **5**: p. 3157.

43. Li, J.F., et al., *Multiplex and homologous recombination-mediated genome editing in Arabidopsis and Nicotiana benthamiana using guide RNA and Cas9.* Nat Biotechnol, 2013. **31**(8): p. 688-91.

44. Rong, Z., et al., *Homologous recombination in human embryonic stem cells using CRISPR/Cas9 nickase and a long DNA donor template.* Protein Cell, 2014. **5**(4): p. 258-60.

45. Upadhyay, S.K., et al., *RNA-guided genome editing for target gene mutations in wheat.* G3 (Bethesda), 2013. **3**(12): p. 2233-8.

46. Cox, D.B., R.J. Platt, and F. Zhang, *Therapeutic genome editing: prospects and challenges.* Nat Med, 2015. **21**(2): p. 121-31.

47. Shan, Q., et al., *Genome editing in rice and wheat using the CRISPR/Cas system.* Nat Protoc, 2014. **9**(10): p. 2395-410.

48. Chu, V.T., et al., *Increasing the efficiency of homology-directed repair for CRISPR-Cas9-induced precise gene editing in mammalian cells.* Nat Biotechnol, 2015. **33**(5): p. 543-8.

49. Maruyama, T., et al., *Increasing the efficiency of precise genome editing with CRISPR-Cas9 by inhibition of nonhomologous end joining.* Nat Biotechnol, 2015. **33**(5): p. 538-42.

50. Robert, F., et al., *Pharmacological inhibition of DNA-PK stimulates Cas9-mediated genome editing.* Genome Med, 2015. **7**(1): p. 93.

51. Pinder, J., J. Salsman, and G. Dellaire, *Nuclear domain 'knock-in' screen for the evaluation and identification of small molecule enhancers of CRISPR-based genome editing.* Nucleic Acids Res, 2015. **43**(19): p. 9379-92.

52. Song, J., et al., *RS-1 enhances CRISPR/Cas9- and TALEN-mediated knock-in efficiency.* Nat Commun, 2016. **7**: p. 10548.

53. Ma, X., et al., *Small molecules promote CRISPR-Cpf1-mediated genome editing in human pluripotent stem cells.* Nat Commun, 2018. **9**(1): p. 1303.

54. Lin, S., et al., *Enhanced homology-directed human genome engineering by controlled timing of CRISPR/Cas9 delivery.* Elife, 2014. **3**: p. e04766.

55. Clementi, M.E., et al., *Antibodies against small molecules.* Ann Ist Super Sanita, 1991. **27**(1): p. 139-43.

56. Yang, N.J. and M.J. Hinner, *Getting across the cell membrane: an overview for small molecules, peptides, and proteins.* Methods Mol Biol, 2015. **1266**: p. 29-53.

57. Kweon, J., et al., *A CRISPR-based base-editing screen for the functional assessment of BRCA1 variants.* Oncogene, 2020. **39**(1): p. 30-35.

58. Inglese, J., et al., *Quantitative high-throughput screening: a titration-based approach that efficiently identifies biological activities in large chemical libraries.* Proc Natl Acad Sci U S A, 2006. **103**(31): p. 11473-8.

59. Macarrón, R. and R.P. Hertzberg, *Design and implementation of high throughput screening assays.* Mol Biotechnol, 2011. **47**(3): p. 270-85.

60. Kim, D., et al., *Genome-wide target specificity of CRISPR RNA-guided adenine base editors.* Nat Biotechnol, 2019. **37**(4): p. 430-435.

61. Hwang, G.H., et al., *Web-based design and analysis tools for CRISPR base editing.* BMC Bioinformatics, 2018. **19**(1): p. 542.

62. Elmer, JJ., et al., *The histone deacetylase inhibitor Entinostat enhances polymer-mediated transgene expression in cancer cell lines.* Biotechnol Bioeng, 2016. **113**(6): p. 1345-1356.

63. Lai, M.D., et al., *An HDAC inhibitor enhances the antitumor activity of a CMV promoter-driven DNA vaccine.* Cancer Gene Ther, 2010. **17**(3): p. 203-11.

64. Tiffon, C., et al., *The histone deacetylase inhibitors vorinostat and romidepsin downmodulate IL-10 expression in cutaneous T-cell lymphoma cells.* Br J Pharmacol, 2011. **162**(7): p. 1590-602.

65. Yen, M.C., et al., *An HDAC inhibitor enhances cancer therapeutic efficiency of RNA polymerase III promoter-driven IDO shRNA.* Cancer Gene Ther, 2013. **20**(6): p. 351-7.

66. Chen, X., et al., *The Chromatin Structure Differentially Impacts High-Specificity CRISPR-Cas9 Nuclease Strategies.* Mol Ther Nucleic Acids, 2017. **8**: p. 558-563.

67. Chen, X., et al., *Probing the impact of chromatin conformation on genome editing tools.* Nucleic Acids Res, 2016. **44**(13): p. 6482-92.

68. Horlbeck, M.A., et al., *Nucleosomes impede Cas9 access to DNA in vivo and in vitro.* Elife, 2016. **5**.

69. Kallimasioti-Pazi, E.M., et al., *Heterochromatin delays CRISPR-Cas9 mutagenesis but does not influence the outcome of mutagenic DNA repair.* PLoS Biol, 2018. **16**(12): p. e2005595.

70. Yarrington, R.M., et al., *Nucleosomes inhibit target cleavage by CRISPR-Cas9 in vivo.* Proc Natl Acad Sci U S A, 2018. **115**(38): p. 9351-9358.

71. Roos, W.P. and A. Krumm, *The multifaceted influence of histone deacetylases on DNA damage signalling and DNA repair.* Nucleic Acids Res, 2016. **44**(21): p. 10017-10030.

72. Jensen, K.T., et al., *Chromatin accessibility and guide sequence secondary structure affect CRISPR-Cas9 gene editing efficiency.* FEBS Lett, 2017. **591**(13): p. 1892-1901.

73. Liu, B., et al., *Inhibition of histone deacetylase 1 (HDAC1) and HDAC2 enhances CRISPR/Cas9 genome editing.* Nucleic Acids Res, 2020. **48**(2): p. 517-532.

74. Iveland, T.S., et al., *HDACi mediate UNG2 depletion, dysregulated genomic uracil and altered expression of oncoproteins and tumor suppressors in B- and T-cell lines.* J Transl Med, 2020. **18**(1): p. 159.

75. Zhao, T., et al., *Small-molecule compounds boost genome-editing efficiency of cytosine base editor.* Nucleic Acids Res, 2021. **49**(15): p. 8974-8986.

76. Liu, N., et al., *HDAC inhibitors improve CRISPR-Cas9 mediated prime editing and base editing.* Mol Ther Nucleic Acids, 2022. **29**: p. 36-46.

국문요약

Clustered regular interspaced short palindromic repeats (CRISPR)-CRISPR-associated protein 9 (Cas9) 시스템은 원래 바이러스 게놈을 방어하기 위한 적응 면역 시스템으로 설계되었으며, 이제는 RNA-guide engineered nuclease (RGENs)으로 불리는 게놈 편집 도구로 더 잘 알려져 있다. CRISPR-Cas9 시스템의 기작은 Cas9 단백질과 gRNA 가 복합체를 형성하여 표적 DNA 서열을 인식하고 DNA 의 이중 가닥 손상 (DSB, double strand break)을 한다. 절단된 DNA 는 세포 내 DNA 복구 경로인 비상동말단연결 (NHEJ. Non-homologous end joining) 또는 상동성 유도 복구 (HDR, Homology-directed repair)를 통해 복구된다. NHEJ 는 작은 삽입과 결실을 통해 유전자 파괴를 유도하는 반면 HDR 은 기증자 주형의 존재 하에서 상동 재조합을 유도하여 유전자 수정과 삽입을 돕는다. 최근 CRISPR 기반 게놈 편집은 농업, 신약 개발, 의학, 생명 공학 등 다양한 분야에서 응용되고 있다. 특히 질병을 치료하는 유망한 도구로 주목받고 있으며 현재 임상시험을 위한 개발이 가속화되고 있다. 이러한 CRISPR 기술이 질병을 치료할 수 있는 큰 잠재력을 가짐에도 불구하고 몇 가지 우려되는 문제가 있다. 최근에는 Cas9 기반 게놈 편집에 따른 DSB 에 의해 p53 매개 세포 독성, 대규모 염색체 결실 및 재배열, 원하지 않는 부산물 및 인델 (Indel, insertion and deletion)의 발생이 지속적으로 보고되고 있다. 또한 많은 병원성 유전 질환이 점 돌연변이에 의해 발생하기 때문에 Cas9 뉴클레아제를 기반으로 한 유전 질환 관련 돌연변이 교정은 비효율적이며 안전성 문제가 있다. 이와 같이 표적 염기를 정밀하게 교정하는 전략을 필요로 했고 DSB 없이 염기를 교정할 수 있는 염기 편집기 (BE, base editor)의 개발이 요구되었다. 염기 편집기는 현재 사이토신 기본 편집기 (CBE, cytosine base editor)와 아데닌 기본 편집기 (ABE, adenine base editor)의 두 가지

유형이 있다. nCas9 에 시토신 탈아미노화효소 (cytidine deaminase) 와 융합된 CBE (nickase Cas9, 촉매적으로 불활성인 D10A 돌연변이)는 C:G 에서 T:A 로의 전환을 유도하고, ABE 는 nCas9 에 대한 아데닌 탈아미노화효소 (adenine deaminase)와 융합되어 A:T 에서 G:C 로의 전환을 유도한다. 현재 세대의 염기 편집기는 효율성을 최적화하기 위해 진화하고 개선되었지만 그 활동은 세포 유형 및 대상 시퀀스에 따라 매우 다양하다. 이전 연구에서는 염기 편집기의 효율성을 개선하기 위한 여러 노력들이 있었다. 특히, 우라실 N-글리코실라아제 (UNG, uracil DNA glycosylase)의 활성을 억제하는 우라실 글리코실라아제 억제제 (UGI, uracil DNA glycosylase inhibitor)를 융합하여 CBE 의 효율이 개선되었다. 따라서 본 연구에서는 특정 내인성 단백질 기능 억제가 염기 편집기에 미치는 효과를 조사하고자 하였다. 특정 단백질 기능을 억제하기 위해 소분자 약물이 적용되었으며 이러한 전략은 Cas9 기반 게놈 편집의 효율성을 향상시키는 데 사용되었지만 아직까지는 염기 편집기에서는 그 효과가 조사되지 않았다. 따라서 이 연구에서는 염기 편집기 효율성에 영향을 미치는 새로운 소분자를 식별하기 위해 형광 기반 리포터 시스템을 개발했다. 리포터 시스템이 통합된 HAP1 세포주에서 항암 특성을 가진 414 개의 소분자 약물 라이브러리를 스크리닝 했고, 히스톤 탈아세틸화효소 (HDAC, Histone deacetylase) 억제제가 높은 순위에 기록되었다. 순위가 가장 높은 로미뎁신은 내인성 표적 부위에서 아데닌 염기 편집 효율을 최대 3.8 배까지 증가시켰다. 이러한 효과는 로미뎁신이 ABE7.10 단백질 및 gRNA 의 발현 수준의 향상에 기여함을 확인하였다. 또한 HDAC 억제제는 히스톤 과아세틸화를 통해 열린 염색질 상태로 전환시킬 수 있다. 따라서 ABE7.10 의 접근성이 향상되었을 거라 추측했고, 발현 강화 효과를 배제하기 위해 정제된 ABE7.10 단백질-gRNA 복합체인 RNP (ribonucleoprotein)을 전기 천공 후 로미뎁신을 처리했을 때 염기 편집 효율이 최대 4.9 배 증가했다. 이러한 결과는 ChIP 분석에 의해 염색질이 열린 상태로 전환됨에 따라 RNP 접근성 향상에 의해 염기 편집 효율이

향상되었음을 시사한다. 결론적으로 HDAC 억제제는 개선된 발현 및 향상된 RNP 접근성을 기반으로 CRISPR 매개 염기 편집의 효율성을 높일 수 있다. 또한 이러한 결과는 CRISPR 매개 게놈 편집의 효율성을 개선하기 위한 추가 연구에 대한 통찰력을 제공하고, 치료 응용 분야에서 생체 내 게놈 편집의 효율성을 높이기 위한 전략을 지원할 수 있다.

keyword: 크리스퍼, 염기 편집기, 아데닌 염기 편집기, 히스톤 탈아세틸화효소 억제제, 로미뎁신